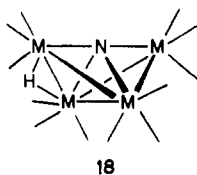


bond is formed. The product of this conversion, **19**, contains a  $\mu_3$ -NH ligand bridging a  $\text{FeRu}_2$  face. By reinsertion into either one of the equivalent Fe–Ru bonds, **19** is converted directly into **20**. Note that these steps not only allow us to obtain a product with the N inserted into a Fe–Ru bond, but they also predict the correct relative positions of the  $\text{Ru}(\text{CO})_3$  and two  $\text{Ru}(\text{CO})_2[\text{P}(\text{OCH}_3)_3]$  groups.

It is reasonable that the last step in the process, the migration of the hydrogen from the nitrogen to the hinge M–M bond, would first involve a bridge between the N and the wing-tip metal, such as depicted in **14**. The next step in the route would involve a shift to the structure shown in **18**, followed by the final migration to the hinge M–M bond. The existence of one structurally char-



acterized butterfly nitrido cluster that does contain a hydrogen bridging a wing-tip to the hinge M–M bond<sup>16</sup> supports the viability of **18** as an intermediate. Perhaps the most important precedent for the N–H to M–H conversion is the fluxional process observed in  $\text{HFe}_4(\text{CH})(\text{CO})_{12}$ , **15**. Using spin saturation transfer techniques, the two hydrogens were found to undergo *intramolecular* exchange.<sup>32</sup>

In the homonuclear cluster,  $[\text{Ru}_4\text{N}(\text{CO})_{12}]^{1-}$ , there is no need for such an elaborate scheme to describe the mechanism of product formation. Proton migration can occur from the intermediate,  $\text{Ru}_4(\text{NH})(\text{CO})_{12}$ , directly to the neutral nitrido product. For

$[\text{FeRu}_3\text{N}(\text{CO})_{12}]^{1-}$ , the predominant isomer in solution contains the iron in the wing-tip position<sup>6</sup> and therefore requires no rearrangement of the metals upon protonation to yield  $\text{HFeRu}_3\text{N}(\text{CO})_{12}$ . Once the isomer with the Fe in the hinge position is protonated, it would have to proceed in a path similar to that described for  $[\text{FeRu}_3\text{N}(\text{CO})_{10}[\text{P}(\text{OCH}_3)_3]_2]^{1-}$  before reaching the correct form of the product.

In the three anions studied, there are only three different  $\text{ML}_3$  groups:  $\text{Fe}(\text{CO})_3$ ,  $\text{Ru}(\text{CO})_3$ , and  $\text{Ru}(\text{CO})_2[\text{P}(\text{OCH}_3)_3]$ . To eq 1–3, we can add the results of the study of  $[\text{Fe}_4\text{N}(\text{CO})_{12}]^{1-}$  which rapidly protonates directly to  $\text{HFe}_4\text{N}(\text{CO})_{12}$  even at low temperatures under CO (i.e., too fast to observe or even trap any intermediates). From these studies, we infer that the rate of conversion from the imido intermediate to the final hydrido product is dependent on the nature of the wing-tip  $\text{ML}_3$  group, with the rate decreasing in the order  $\text{Fe}(\text{CO})_3 > \text{Ru}(\text{CO})_3 > \text{Ru}(\text{CO})_2[\text{P}(\text{OCH}_3)_3]$ .

**Acknowledgment.** We gratefully acknowledge the National Science Foundation for supporting this research.

**Registry No.** 1, 84549-71-3; 2, 90968-69-7; 3, 100927-51-3; 4, 76791-95-2; 5-PPN, 100927-53-5; 5- $\text{Et}_4\text{N}$ , 100927-57-9; 6, 100938-64-5; 7, 100927-54-6; 8, 100938-65-6; 9, 100938-66-7; 12, 100938-67-8; 13, 100927-55-7;  $\text{Ru}_3(\text{CO})_{12}$ , 15243-33-1; PPN $[\text{FeRu}_4\text{N}(\text{CO})_{14}]$ , 90990-44-6; PPN $[\text{Ru}_4\text{N}(\text{CO})_{12}]$ , 92845-78-8; PPN $[\text{Ru}_5\text{N}(\text{CO})_{14}]$ , 83312-28-1;  $\text{HFeRu}_3\text{N}(\text{CO})_{11}[\text{P}(\text{OCH}_3)_3]$ , 100927-56-8; Fe, 7439-89-6; Ru, 7440-18-8.

**Supplementary Material Available:** A listing of the structure factors and thermal parameters for both of the structures (15 pages). Ordering information can be found on any current masthead page.

## Epoxidation of Olefins with Cationic (salen) $\text{Mn}^{\text{III}}$ Complexes. The Modulation of Catalytic Activity by Substituents

K. Srinivasan, P. Michaud, and J. K. Kochi\*

Contribution from the Department of Chemistry, University of Houston, University Park, Houston, Texas 77004. Received August 28, 1985

**Abstract:** Cationic manganese(III) complexes of the salen ligand [*N,N'*-ethylenebis(salicylideneaminato)] are effective catalysts for the epoxidation of various olefins with iodosylbenzene as the terminal oxidant. The presence of electron-withdrawing groups, such as 5,5'-dichloro or -dinitro substituents, enhances the catalytic activity of the (salen) $\text{Mn}^{\text{III}}$  catalyst in measure with the electron-deficient character of the cationic complex as evaluated by the standard reduction potential  $E^\circ$ . Various types of olefins, including substituted styrenes, stilbenes, and cyclic and acyclic alkenes, are epoxidized in 50–75% yields within 15 min at ambient temperatures in acetonitrile. Stereospecific epoxidation is achieved with *trans*-olefins such as (*E*)-2-hexene and (*E*)- $\beta$ -methylstyrene. *cis*-Olefins produce high yields of *cis*-epoxides which contain minor amounts of the corresponding *trans* isomer. Competition from allylic oxidation is minor with this catalyst system—cyclohexene being converted selectively to its epoxide accompanied by only traces of cyclohexenol. Competition studies indicate that the relative reactivity of olefins toward catalytic epoxidation with the cationic (salen) $\text{Mn}^{\text{III}}$  complexes falls into an unusually narrow range, the difference between the most reactive, *p*-methoxystyrene, and the least reactive, 1-octene, being only a factor of 10. The effect of donor ligands such as pyridine and imidazole is discussed in the context of a radical-like behavior of an oxomanganese species as the reactive intermediate. The latter is supported by some preliminary studies of alkane oxidation using cyclohexane as a model.

Metal catalysis of the oxidation of various organic substrates is of synthetic as well as of biochemical interest.<sup>1</sup> In our earlier study of the chromium-catalyzed epoxidation of olefins, we showed how oxochromium(V) species play a critical role in the catalytic cycle.<sup>2,3</sup> The successful isolation and determination of the X-ray

crystal structure of the reactive oxochromium(V) intermediates were allowed by the use of the salen [*N,N'*-ethylenebis(salicylideneaminato)] ligand. Indeed as a ligand, salen has the desirable characteristic of being readily subject to systematic modification of its electronic and steric properties. In particular, substituents on the 5-positions which are para to the pair of ligating oxygen atoms strongly perturb the redox properties of (salen)metal

(1) Sheldon, R. A.; Kochi, J. K. "Metal-Catalyzed Oxidations of Organic Compounds"; Academic: New York, 1981.

(2) Siddall, T. L.; Miyaura, N.; Huffman, J. C.; Kochi, J. K. *J. Chem. Soc., Chem. Commun.* 1983, 1185.

(3) Samsel, E. G.; Srinivasan, K.; Kochi, J. K. *J. Am. Chem. Soc.* 1985, 107, 7606.

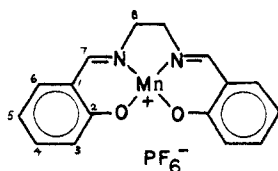
complexes.<sup>4</sup> The steric properties of (salen)metal complexes are modulated by the presence of substituents on the ethano (i.e., 8-position) bridge.<sup>5</sup>

Although chromium complexes are useful for mechanistic studies to demonstrate the role of the oxometal intermediate, their utility as catalysts for general epoxidation is unfortunately limited to electron-rich olefins. Most seriously, acyclic alkenes such as 1- and 2-octenes are essentially unaffected by this catalytic system. Accordingly we have turned our attention to other (salen)metal analogues which are significantly more reactive than their chromium counterparts.

We now report the unusual reactivity of manganese salen complexes in which the active oxomanganese species appears only as a fleeting putative intermediate. As a result, we have depended on indirect methods to probe the nature of the oxygen-atom transfer to the olefinic substrate. The relationship of this catalytic system to the biochemically relevant manganese porphyrins<sup>6-10</sup> is an important consideration. We have used iodosylbenzene as the terminal oxidant in these studies owing to its limited solubility in either methylene chloride or acetonitrile.<sup>11</sup>

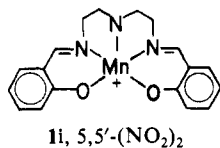
## Results

**I. Synthesis and Structure of the (salen)Mn Catalysts.** The manganese catalysts used in this study derive from a series of cationic salen complexes **1a-h** of the general structure



- 1a**, unsubstituted  
**b**, 3,3'-(MeO)<sub>2</sub>  
**c**, 5,5'-(MeO)<sub>2</sub>  
**d**, 7,7'-(C<sub>6</sub>H<sub>5</sub>)<sub>2</sub>  
**e**, 5,5'-Cl<sub>2</sub>  
**f**, 5,5'-(NO<sub>2</sub>)<sub>2</sub>  
**g**, 5,5'-(NO<sub>2</sub>)<sub>2</sub>-8,8,8',8'-(CH<sub>3</sub>)<sub>4</sub>  
**h**, 3,3',5,5'-(NO<sub>2</sub>)<sub>4</sub>

together with a derivative of the pentacoordinating ligand **saldien**.<sup>12</sup>



**1i**, 5,5'-(NO<sub>2</sub>)<sub>2</sub>

(4) Cf.: (a) Coleman, W. M.; Boggess, R. K.; Hughes, J. W.; Taylor, L. T. *Inorg. Chem.* **1981**, *20*, 700. (b) Coleman, W. M.; Boggess, R. K.; Hughes, J. W.; Taylor, L. T. *Inorg. Chem.* **1981**, *20*, 1253. (c) Coleman, W. M.; Goehring, R. R.; Taylor, L. T.; Mason, J. G.; Boggess, R. K. *J. Am. Chem. Soc.* **1979**, *101*, 2311. (d) See also: Earnshaw, A.; King, E. A.; Larkworthy, L. F. *J. Chem. Soc. A* **1968**, 1048.

(5) Srinivasan, K.; Kochi, J. K. *Inorg. Chem.* **1985**, *24*, 4671.

(6) Groves, J. T.; Kruper, W. J., Jr.; Haushalter, R. C. *J. Am. Chem. Soc.* **1980**, *102*, 6377.

(7) Hill, C. L.; Schardt, B. C. *J. Am. Chem. Soc.* **1980**, *102*, 6374.

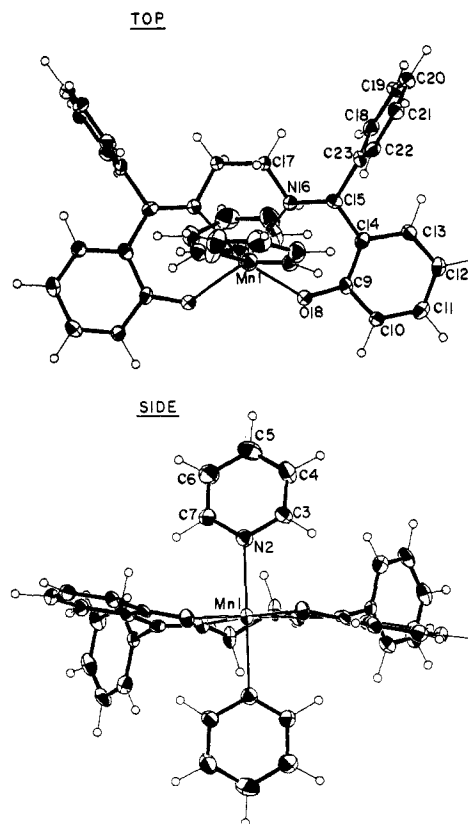
(8) (a) Guilmet, E.; Meunier, B. *Nouv. J. Chim.* **1982**, *6*, 511. (b) Collman, J. P.; Kodadek, T.; Raybuck, S. A.; Meunier, B. *Proc. Natl. Acad. Sci. U.S.A.* **1985**, *80*, 7039. (c) Meunier, B.; Guilmet, E.; De Carvalho, M.-E.; Poilblanc, R. *J. Am. Chem. Soc.* **1984**, *106*, 6668. (d) Collman, J. P.; Brauman, J. I.; Meunier, B.; Raybuck, S. A.; Kodadek, T. *Proc. Natl. Acad. Sci. U.S.A.* **1984**, *81*, 3245. (e) Collman, J. P.; Brauman, J. I.; Meunier, B.; Hayashi, T.; Kodadek, T.; Raybuck, S. A. *J. Am. Chem. Soc.* **1985**, *107*, 2000.

(9) See also: (a) Tabushi, I.; Yazaki, A. *J. Am. Chem. Soc.* **1981**, *103*, 7371. (b) Ehrenfeld, G. M.; Murugesan, N.; Hecht, S. M. *Inorg. Chem.* **1984**, *23*, 1498. (c) van der Made, A. W.; Smeets, J. W. H.; Nolte, R. J. M.; Drenth, W. *J. Chem. Soc., Chem. Commun.* **1983**, 1204. (d) Powell, M. F.; Pai, E. F.; Bruce, T. C. *J. Am. Chem. Soc.* **1984**, *106*, 3277.

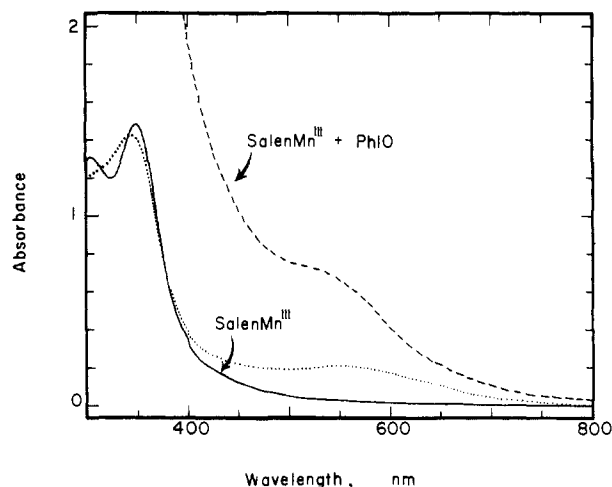
(10) (a) Mansuy, D.; Battioni, P.; Renaud, J.-P. *J. Chem. Soc., Chem. Commun.* **1984**, 1255. (b) Renaud, J.-P.; Battioni, P.; Bartoli, J. F.; Mansuy, D. *J. Chem. Soc., Chem. Commun.* **1985**, 888. (c) Mansuy, D.; Fontecave, M.; Bartoli, J.-F. *J. Chem. Soc., Chem. Commun.* **1983**, 253.

(11) Although the solubility of iodosylbenzene in acetonitrile is <10<sup>-4</sup> mM, the rate of oxygen-atom transfer is sufficiently fast to allow solubilization within 5-10 min in an active catalytic system.

(12) (salen)Mn<sup>III</sup> complexes are isolated either as the hydrate or alcoholate with hexafluorophosphate as the counterion.



**Figure 1.** ORTEP diagram of (7,7'-Ph)salenMn(py)<sub>2</sub> shown in top and side perspectives. Only half the atoms are numbered, the mirrored atoms to be designated with primes.



**Figure 2.** Absorption spectrum of  $2 \times 10^{-3}$  M [(5,5'-(NO<sub>2</sub>)<sub>2</sub>salen)]-Mn<sup>+</sup>PF<sub>6</sub><sup>-</sup> in acetonitrile taken in a 1-mm cuvette. The dashed curve is the same solution immediately after reaction with excess iodosylbenzene, the dotted curve after a 4-fold dilution.

**Table I.** Reduction Potentials of (salen)Mn<sup>III</sup> Cations<sup>a</sup>

(salen)Mn <sup>III</sup>	E° V vs. SCE	(salen)Mn <sup>III</sup>	E° V vs. SCE
unsubstituted	-0.44	5,5'-dichloro	-0.34
3,3'-dimethoxy	-0.42	5,5'-dinitro	-0.07
7,7'-diphenyl	-0.47	3,3',5,5'-tetranitro	+0.25

<sup>a</sup> Cyclic voltammetric measurements performed on  $1 \times 10^{-3}$  M [(salen)Mn]<sup>+</sup>PF<sub>6</sub><sup>-</sup> in dimethyl sulfoxide containing 0.1 M tetra-*n*-butylammonium hexafluorophosphate at 25 °C. Potentials calibrated with respect to ferrocene E° 0.31 V.<sup>15</sup>

These (salen)Mn<sup>III</sup> cations were synthesized from the corresponding (salen)Mn<sup>II</sup> complexes by electron transfer to outer-sphere oxidants such as ferrocenium, tris(phenanthroline)iron(III),

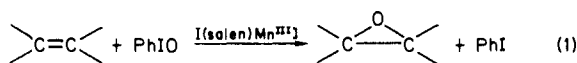
Table II. Effect of Catalyst Structure on the Epoxidation of Cyclohexene and 1-Octene<sup>a</sup>

(salen)Mn <sup>III</sup>	cyclohexene		1-octene epoxide, mmol (%)
	epoxide, mmol (%)	alcohol, <sup>b</sup> mmol (%)	
5,5'-dimethoxy	0.053 (36)	tr	0.018 (12)
3,3'-dimethoxy	0.083 (56)	tr	0.036 (25)
7,7'-diphenyl	0.059 (40)	tr	0.022 (15)
5,5'-dichloro	0.083 (57)	0.004 (3)	0.060 (41)
5,5'-dinitro	0.105 (67)	0.006 (4)	0.089 (59)
	0.070 (46) <sup>c</sup>	0.003 (2) <sup>d</sup>	
3,3',5,5'-tetranitro	0.088 (61)	<i>e</i>	<i>f</i>
5,5'-dinitro <sup>g</sup>	<i>f</i>	<i>f</i>	0.077 (52)

<sup>a</sup>In 5 mL of acetonitrile containing 0.011 mmol of (salen)Mn<sup>III</sup> catalyst, 0.15 mmol of iodosylbenzene, and 0.30 mmol of olefin at 25 °C. Percent yields expressed relative to PhI formed. <sup>b</sup>2-Cyclohexenol; tr = traces (<0.5%). <sup>c</sup>Reaction in 5 mL of methanol; 0.084 mmol of cyclohexene consumed. <sup>d</sup>Cyclohexenyl methyl ether. <sup>e</sup>Traces in addition to other minor byproducts (see Experimental Section). <sup>f</sup>Not determined. <sup>g</sup>saldien complex **1i**.

and tris(bipyridine)iron(III) hexafluorophosphates. The (salen)Mn<sup>II</sup> complexes are air-sensitive, yellow or orange solids which are sparingly soluble in acetonitrile.<sup>13</sup> However, the 7,7'-diphenyl derivative is soluble in pyridine, and the ORTEP diagram from the X-ray crystallography of the bis(pyridine) adduct is shown in Figure 1. Unlike their manganese(II) counterparts, the complexes **1a-i** are all readily soluble in acetonitrile. The electronic spectra of these clear brown solutions are characterized by absorption bands with  $\lambda_{\max} \sim 350$  nm tailing to beyond 400 nm, as typically shown in Figure 2. The redox properties of the cationic (salen)Mn<sup>III</sup> complex are strongly dependent on substituents. Thus, the reversible reduction potential obtained by cyclic voltammetry is increased by  $\sim 700$  mV upon substitution by a pair of 3,5-dinitro groups (Table I).

**II. Activity of (salen)Mn<sup>III</sup> Cations in Olefin Epoxidation with Iodosylbenzene.** When a clear brown solution of (salen)Mn<sup>III</sup> in acetonitrile is treated with iodosylbenzene, it immediately turns dark. The appearance of a new absorption band (with  $\lambda_{\max} \sim 530$  in Figure 2) is strongly reminiscent of the spectral change obtained during the conversion of the related (salen)Cr<sup>III</sup> cation to the corresponding oxochromium(V) species under the same conditions.<sup>3</sup> Upon standing, the dark brown solution fades to the original light brown within 2–3 h. When the same experiment is carried out in the presence of norbornene, the dark brown is immediately discharged to its original hue, and norbornene oxide can be isolated in 70% yield relative to iodobenzene, i.e.,



The absorption spectrum of the final solution coincides with that of the original (salen)Mn<sup>III</sup> catalyst. The epoxidation cycle can be repeated by the addition of more iodosylbenzene. Beyond 30 cycles, however, the catalyst concentration diminishes owing to an irreversible degradation.

**III. Catalytic Epoxidation of Olefins.** The efficacy of various salen ligands was investigated under a standard set of conditions by using catalytic amounts of the corresponding manganese(III) complex together with cyclohexene and 1-octene as the test olefins. The results listed in Table II indicate that the different (salen)-Mn<sup>III</sup> catalysts are not strongly differentiated in their ability to generate cyclohexene oxide. With each catalyst, cyclohexene is cleanly converted to its epoxide with only traces of allylic oxidation to cyclohexenol. However, the epoxidation of 1-octene is more dependent on the catalyst structure. Thus, those salen complexes

with electron-releasing substituents such as the 5,5'-dimethoxy and 7,7'-diphenyl derivatives effect only poor yields of 1-octene oxide, whereas those with 5,5'-dichloro and 5,5'-dinitro substituents lead to the best epoxide yields. In each case the iodosylbenzene charged was converted to iodobenzene in >90%.

The catalytic epoxidation of cyclohexene was also examined in methylene chloride. In this noncoordinating solvent, the (5,5'-(NO<sub>2</sub>)<sub>2</sub>salen)Mn<sup>III</sup> catalyst **1f** is only sparingly soluble and affords a turbid khaki-colored mixture. Addition of iodosylbenzene and cyclohexene in the quantities listed in Table II yielded a heterogeneous mixture which slowly reacted over a period of  $\sim 5$  h to yield 57% cyclohexene oxide, 1.4% cyclohexenol, and 3% cyclohexenone. Owing to the slow, heterogeneous character of this system, we carried out all further epoxidation studies in acetonitrile.

Since high yields of cyclohexene and octene oxides were obtained with the (5,5'-(NO<sub>2</sub>)<sub>2</sub>salen)Mn<sup>III</sup> catalyst **1f**, we examined its effect on a structurally diverse series of olefins listed in Table III. The olefin consumed during the epoxidation was determined as the difference between the amount charged and that recovered. On this basis, many olefins are converted efficiently to the corresponding epoxide, the styrenes being the outstanding exceptions probably as a result of partial polymerization. The yields of epoxides in Table III were calculated on the basis of the amount of iodobenzene formed. Since the latter also proceeds competitively in the absence of an olefin substrate,<sup>16</sup> the listed yields largely reflect the relative reactivity of the olefin. All of the epoxidations are complete within 30 min, at 25 °C. In order to test the reliability of the results obtained with the (5,5'-(NO<sub>2</sub>)<sub>2</sub>salen)Mn<sup>III</sup> catalyst (particularly with respect to the byproducts), the epoxidations of some of the olefins were reexamined with the less reactive parent cation **1a**. Essentially the same results as those listed in Table III were obtained (see Experimental Section).

The formation of byproducts during the catalytic epoxidation (see Table III) is noteworthy. Although the amounts of byproducts are by and large minor, control experiments establish that they are mostly formed during the course of epoxidation and not from the subsequent rearrangement of the epoxide. For example, styrene oxide added to a mixture consisting of 1-octene, iodosylbenzene, and **1f** was quantitatively recovered intact after the epoxidation was complete. (See Experimental Section for details.) The same was true of (*Z*)- $\beta$ -methylstyrene oxide when **1a** was used as the catalyst under the same conditions.  $\alpha$ -Methylstyrene oxide was also stable to epoxidation conditions when imidazole was present with **1a**; otherwise, it was partially converted to  $\alpha$ -phenylpropionaldehyde. Neither deoxybenzoin nor diphenylacetaldehyde (see Tables III and IV) is a product of rearrangement of either (*Z*)- or (*E*)-stilbene oxide. However, the highly labile *p*-methoxystyrene oxide undergoes complete rearrangement to *p*-methoxyphenylacetaldehyde under reaction conditions. Thus, in this case, we were unable to establish whether the principal product *p*-methoxyphenylacetaldehyde was a primary result of catalytic epoxidation or derived from the subsequent rearrangement of the first-formed epoxide, or both.

The stereochemistry of oxygen-atom transfer is shown in Table III by the formation of epoxides with little or no isomerization. Thus, the *E* isomers of 2-hexene, stilbene, and  $\beta$ -methylstyrene by and large afford only *trans*-epoxides. Since the *Z* isomers produced minor amounts of (*E*)-epoxides, we examined the effect of the catalyst structure on the stereospecificity of epoxidation. The results with (*Z*)- $\beta$ -methylstyrene are given in Table IV. Control experiments established that the minor amounts of the byproduct phenylacetone were not a result of the rearrangement of either (*E*)- or (*Z*)- $\beta$ -methylstyrene oxide.

The effect of donor ligands on the catalytic epoxidation of 1-octene is shown in Table V. Thus, the addition of relatively small amounts (5–10 equiv) of pyridine and pyridine *N*-oxide leads to increased yields of 1-octene oxide. However, the presence of

(13) Owing to intermolecular coordination through the oxygen of a neighboring (salen)Mn<sup>II</sup>. Consequently they are usually soluble in donor solvents such as dimethyl sulfoxide.

(14) (a) Calligaris, M.; Nardin, G.; Radaccio, L. *Coord. Chem. Rev.* **1972**, *7*, 385. (b) Hobday, M. D.; Smith, T. D. *Coord. Chem. Rev.* **1973**, *9*, 311.

(15) Gagne, R. R.; Koval, C. A.; Lisensky, G. C. *Inorg. Chem.* **1980**, *19*, 2854.

(16) The oxidation products derived from the manganese(III) catalysis of iodosylbenzene decomposition in the absence of olefin will be reported separately.

**Table III.** Epoxides from Olefins with Iodosylbenzene Catalyzed by (5,5'-(NO<sub>2</sub>)<sub>2</sub>salen)Mn<sup>III</sup><sup>a</sup>

olefin	olefin consumed, mmol	epoxide, mmol (%)	other products, mmol (%)
PhCH=CH <sub>2</sub>	0.13	0.054 (37)	PhCH <sub>2</sub> CHO 0.014 (10)
4-MeC <sub>6</sub> H <sub>4</sub> CH=CH <sub>2</sub>	0.13	0.044 (30)	ArCH <sub>2</sub> CHO 0.029 (20)
4-MeOC <sub>6</sub> H <sub>4</sub> CH=CH <sub>2</sub>	0.16	<i>b</i>	ArCH <sub>2</sub> CHO 0.073 (48)
4-ClC <sub>6</sub> H <sub>4</sub> CH=CH <sub>2</sub>	0.13	0.077 (48)	ArCH <sub>2</sub> CHO 0.015 (9)
PhC(CH <sub>3</sub> )=CH <sub>2</sub>	0.141	0.071 (45)	PhCH(CH <sub>3</sub> )CHO 0.058 (27)
2,6-(CH <sub>3</sub> ) <sub>2</sub> C <sub>6</sub> H <sub>3</sub> CH=CH <sub>2</sub>	<i>c</i>	0.105 (69)	ArCH <sub>2</sub> CHO <0.005
( <i>Z</i> )-PhCH=CHCH <sub>3</sub>	0.14	( <i>Z</i> ) 0.068 (46)	PhCH <sub>2</sub> COCH <sub>3</sub> 0.012 (8)
		( <i>E</i> ) 0.0025 (2)	
( <i>E</i> )-PhCH=CHCH <sub>3</sub>	0.15	( <i>Z</i> ) <0.0001	PhCH <sub>2</sub> COCH <sub>3</sub> <0.001
		( <i>E</i> ) 0.089 (57)	
( <i>Z</i> )-PhCH=CHPh	<i>c</i>	( <i>Z</i> ) 0.045 (31)	PhCH <sub>2</sub> COPh 0.010 (7)
		( <i>E</i> ) 0.006 (4)	Ph <sub>2</sub> CHCHO 0.011 (7)
( <i>E</i> )-PhCH=CHPh	<i>c</i>	( <i>Z</i> ) 0.002 (1)	PhCH <sub>2</sub> COPh 0.010 (7)
		( <i>E</i> ) 0.057 (39)	Ph <sub>2</sub> CHCHO 0.009 (6)
cyclooctene	0.13	0.092 (64)	
( <i>Z</i> )-CH <sub>3</sub> CH <sub>2</sub> CH <sub>2</sub> CH=CHCH <sub>3</sub>	0.15	( <i>Z</i> ) 0.106 (69)	
		( <i>E</i> ) <0.002	
( <i>E</i> )-CH <sub>3</sub> CH <sub>2</sub> CH <sub>2</sub> CH=CHCH <sub>3</sub>	0.14	( <i>Z</i> ) <0.001	
		( <i>E</i> ) 0.070 (50)	
norbornene	0.12	0.084 (56)	

<sup>a</sup> In 5 mL of acetonitrile containing 0.01 mmol of **1f**, 0.15 mmol of iodosylbenzene, and 0.30 mmol of olefin. Percent yields based on PhI formed. <sup>b</sup> Rearrangements under reaction conditions. <sup>c</sup> Not determined.

**Table IV.** Stereospecificity in the Epoxidation of (*Z*)- $\beta$ -Methylstyrene Catalyzed by Various (salen)Mn<sup>III</sup> Complexes<sup>a</sup>

(salen)Mn <sup>III</sup>	epoxide, mmol			<i>Z</i> / <i>E</i> -epoxide
	<i>Z</i>	<i>E</i>	other <sup>b</sup>	
3,3'-dimethoxy	0.033	0.006	<0.001	6
5,5'-dimethoxy	0.033	0.003	0.006	11
unsubstituted	0.051	0.006	0.020	9
5,5'-dichloro	0.058	0.004	0.023	13
5,5'-dinitro	0.068	0.003	0.012	23
5,5'-dinitro <sup>c</sup>	0.073	0.005	0.010	16

<sup>a</sup> In 5 mL of acetonitrile containing 0.30 mmol of (*Z*)- $\beta$ -methylstyrene, 0.15 mmol of iodosylbenzene, and 0.011 mmol of **1** at 25 °C. <sup>b</sup> Phenylacetone. <sup>c</sup> saldien complex **11**.

**Table V.** Effect of Pyridine on the Epoxidation of 1-Octene Catalyzed by the (salen)Mn<sup>III</sup> Complex **1a**

donor ligand, equiv <sup>b</sup>	1-octene oxide, mmol (%) <sup>c</sup>	donor ligand, equiv <sup>b</sup>	1-octene oxide, mmol (%) <sup>c</sup>
py <sup>d</sup>	0	py <sup>d</sup>	15
	0.042 (30)		0.077 (53)
	5		25
	0.081 (56)		0.077 (53)
	10		50
	0.086 (59)		0.062 (42)
pyO <sup>e</sup>	5		100
	0.077 (52)		0.043 (29)
	10		200
	0.074 (51)		0.031 (21)
ImAc <sup>f</sup>	1		
	0.068 (47)		
	10		
	0.022 (15)		

<sup>a</sup> In 5 mL of acetonitrile containing 0.30 mmol of 1-octene, 0.15 mmol of iodosylbenzene, and 0.11 mmol of **1a** at 25 °C. <sup>b</sup> Number of equivalents relative to catalyst. <sup>c</sup> Based on iodobenzene formed. <sup>d</sup> Pyridine. <sup>e</sup> Pyridine *N*-oxide. <sup>f</sup> 4-(Imidazol-1-yl)acetophenone.

large amounts (>25 equiv) of pyridine has a deleterious effect. The donor influence is highly compressed with 4-(imidazol-1-yl)acetophenone,<sup>8</sup> since the addition of only 1 equiv is sufficient to enhance the epoxide yield to 47%, but the presence of 10 equiv deleteriously cuts the yield down to 14%. The donor ligands are less effective with electron-rich olefins such as (*Z*)-stilbene and (*Z*)- $\beta$ -methylstyrene. Essentially no enhancement in epoxide yields is obtained with these olefins when 10 equiv of pyridine is added. Furthermore this donor ligand has no effect on the stereochemical outcome of the epoxidation. It is noteworthy, however, that the amounts of the carbonyl byproducts such as deoxybenzoin and diphenylacetaldehyde are reduced significantly when pyridine is present during epoxidation.

The reactivity of various olefins to catalytic epoxidation was measured by the competition method. Initially we examined the effect of the catalyst structure on the relative reactivity of cy-

**Table VI.** Effect of Catalyst Structure on the Relative Reactivity of Olefins<sup>a</sup>

(salen)Mn <sup>III</sup>	<i>c</i> -C <sub>6</sub> H <sub>10</sub> / 1-C <sub>8</sub> H <sub>16</sub> , <sup>b</sup> mol/mol	epoxide, mmol		rel reactivity <sup>c</sup>
		<i>c</i> -C <sub>6</sub> H <sub>10</sub> O <sup>d</sup>	1-C <sub>8</sub> H <sub>16</sub> O	
unsubst, <b>1a</b>	0.715/0.694	0.069 <sup>e</sup>	0.007	10
	0.469/0.910	0.065 <sup>e</sup>	0.014	9
unsubst/py <sup>f</sup>	0.721/0.704	0.091 <sup>e</sup>	0.009	10
3,3'-(MeO) <sub>2</sub> , <b>1b</b>	0.717/0.681	0.062 <sup>e</sup>	0.008	8
5,5'-Cl <sub>2</sub> , <b>1e</b>	0.712/0.706	0.074 <sup>g</sup>	0.010	8
5,5'-(NO <sub>2</sub> ) <sub>2</sub> , <b>1f</b>	0.738/0.676	0.073 <sup>h</sup>	0.016	5

(salen)Mn <sup>III</sup>	PhC <sub>3</sub> H <sub>5</sub> / <i>c</i> -C <sub>8</sub> H <sub>14</sub> , <sup>i</sup> mol/mol	epoxide, mmol		rel reactivity
		PhC <sub>3</sub> H <sub>5</sub> O	1-C <sub>8</sub> H <sub>14</sub> O	
unsubst, <b>1a</b>	0.904/0.467	0.074	0.021	0.55
	0.685/0.694	0.062	0.028	0.45
	0.455/0.925	0.050	0.046	0.46
5,5'-(NO <sub>2</sub> ) <sub>2</sub> , <b>1f</b>	0.910/0.461	0.096	0.025	0.52
	0.685/0.691	0.078	0.039	0.49
	0.455/0.926	0.069	0.062	0.44

<sup>a</sup> In 5 mL of acetonitrile containing olefins (column 2), 0.011 mmol of catalyst, and PhIO as stated. <sup>b</sup> Cyclohexene/1-octene with 0.18 mmol of PhIO. <sup>c</sup> See Experimental Section for calculation. <sup>d</sup> In addition to cyclohexenol in indicated amounts (mmol). <sup>e</sup> 0.001. <sup>f</sup> 0.011 mmol of pyridine added. <sup>g</sup> 0.003. <sup>h</sup> 0.002. <sup>i</sup> (*E*)- $\beta$ -Methylstyrene/cyclooctene with 0.20 mmol of PhIO.

clohexene and 1-octene. The results in Table VI (upper) indicate that 5-nitro substitution on (salen)Mn<sup>III</sup> leads to the lowest selectivity—it being reduced by a factor of roughly twice beyond that of the other catalysts. The presence of the donor ligand pyridine has no influence on the relative reactivity of (salen)Mn<sup>III</sup> toward cyclohexene and 1-octene. In order to test further the reliability of the competition method, the relative reactivity of cyclooctene and  $\beta$ -methylstyrene was measured at various molar ratios with two catalysts **1a** and **1f**. The comparison in Table VI (lower) indeed shows little differentiation in these systems. Accordingly we undertook an examination of a more extensive series of olefins. The relative reactivities of the olefins listed in Table VII were determined by a competition with styrene. The validity of these values checks successfully with those determined by a direct competition between two olefins.


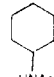
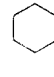
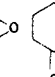
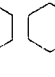
**IV. Manganese Catalysis of Carbon-Hydrogen Activation.** The detailed study of cyclohexene oxidation in Table II reveals the presence of cyclohexenol as a minor but persistent byproduct, the yield of which increases with the electron deficiency of the catalyst. This product of allylic oxidation can be circumvented by the addition of a radical trap such as ionol (2,6-di-*tert*-butyl-*p*-cresol).

Table VII. Relative Reactivities of Olefin in Epoxidation Catalyzed by (5,5'-(NO<sub>2</sub>)<sub>2</sub>salen)Mn<sup>III</sup><sup>a</sup>

olefin	olefin, mmol <sup>b</sup>	PhCH=CH <sub>2</sub> , mmol <sup>b</sup>	olefin, mmol <sup>c</sup>	PhCH=CH <sub>2</sub> , mmol <sup>c</sup>	rel reactivity <sup>d</sup>
<i>p</i> -CH <sub>3</sub> OC <sub>6</sub> H <sub>4</sub> CH=CH <sub>2</sub>	0.290	0.304	0.213	0.249	1.5
<i>p</i> -CH <sub>3</sub> C <sub>6</sub> H <sub>4</sub> CH=CH <sub>2</sub>	0.295	0.301	0.216	0.219	1.0
<i>p</i> -ClC <sub>6</sub> H <sub>4</sub> CH=CH <sub>2</sub>	0.294	0.304	0.234	0.231	0.8
2,6-(CH <sub>3</sub> ) <sub>2</sub> C <sub>6</sub> H <sub>3</sub> CH=CH <sub>2</sub>	0.294	0.296	0.249	0.197	0.4
C <sub>6</sub> H <sub>5</sub> C(CH <sub>3</sub> )=CH <sub>2</sub>	0.282	0.285	0.187	0.207	1.3
( <i>E</i> )-C <sub>6</sub> H <sub>5</sub> CH=CHCH <sub>3</sub>	0.275	0.281	0.214	0.219	1.0
( <i>Z</i> )-C <sub>6</sub> H <sub>5</sub> CH=CHCH <sub>3</sub>	0.270	0.288	0.209	0.223	1.0
cyclohexene	0.300	0.291	0.229	0.224	1.0
cyclooctene	0.230	0.284	0.185	0.188	0.5
CH <sub>3</sub> (CH <sub>2</sub> ) <sub>3</sub> CH=CH <sub>2</sub>	0.231	0.291	0.212	0.164	0.15
( <i>Z</i> )-CH <sub>3</sub> (CH <sub>2</sub> ) <sub>2</sub> CH=CHCH <sub>3</sub>	0.285	0.295	0.231	0.200	0.5
( <i>Z</i> )-CH <sub>3</sub> (CH <sub>2</sub> )CH=CHCH <sub>3</sub>	0.301	0.295 <sup>f</sup>	0.222	0.252 <sup>g</sup>	1.9 <sup>g</sup>
norbornene	0.270	0.280	0.209	0.221	1.1
( <i>Z</i> )-PhCH=CHPh	0.296	0.309	0.209	0.238	1.4
( <i>Z</i> )-PhCH=CHPh	0.295	0.304 <sup>i</sup>	0.215	0.221 <sup>h</sup>	1.0 <sup>j</sup>

<sup>a</sup> In 5 mL of acetonitrile containing 0.15 mmol of PHIO and 0.11 mmol of **1f** at 25 °C. <sup>b</sup> Initial amount. <sup>c</sup> Final amount. <sup>d</sup> See Experimental Section. <sup>e</sup> (*E*)-2-Hexene. <sup>f</sup> (*E*)-2-Hexene oxide. <sup>g</sup> Relative to *E* isomer. <sup>h</sup> (*E*)-Stilbene. <sup>i</sup> (*E*)-Stilbene oxide. <sup>j</sup> Relative to *E* isomer.

Table VIII. Cyclohexane Oxidation Catalyzed by Cationic (salen)Mn<sup>III</sup> Complexes<sup>a</sup>

(salen)Mn <sup>III</sup>					
unsubst, <b>1a</b>	19	23	14	3	4
3,3'-dimethoxy, <b>1b</b>	7	b	3	2	b
5,5'-dichloro, <b>1e</b>	18	16	11	3	4
5,5'-dinitro, <b>1f</b>	23	20	10	3	5
5,5'-dinitro-8,8,8',8'-tetramethyl, <b>1a</b>	9	13	5	2	8
3,3',5,5'-tetranitro, <b>1h</b>	28	19	4	3	9

<sup>a</sup> In 5 mL of acetonitrile containing 600 μL (~5.5 mmol) of cyclohexane, 0.15 mmol of iodosylbenzene, and 0.011 mmol of catalyst at 25 °C. Numbers in the table refer to 10<sup>3</sup> mmol of the product. <sup>b</sup> Traces, <0.0001 mmol.

For example, the presence of 0.1 mmol of ionol during the oxidation of cyclohexene under standard catalytic conditions<sup>17</sup> was sufficient to eliminate cyclohexenol as a byproduct. [Note that in the absence of ionol, 4% cyclohexenol is formed.] There is also a slight diminution in the yield of cyclohexene oxide from 53% to 42%.

The intermediate leading to cyclohexenol can also be diverted by chloride in the form of the soluble, readily dried tetraphenylarsonium salt. Thus, the addition of 0.022 mmol of Ph<sub>4</sub>AsCl to cyclohexene oxidation under standard catalytic conditions<sup>17</sup> afforded 3-chlorocyclohexene in 4% yield in addition to a 39% yield of cyclohexene oxide.

Carbon-hydrogen activation of a saturated hydrocarbon can also be achieved with the (salen)Mn<sup>III</sup> catalyst, similar to those previously investigated with manganese porphyrins.<sup>18</sup> For example, iodosylbenzene disappears at qualitatively the same rate (15–30 min) if cyclohexene is replaced with cyclohexane. Analysis of the oxidation mixture reveals the presence of cyclohexanol, *N*-cyclohexylacetamide, and cyclohexene oxide as the major products formed in ~30% (total) yield. Cyclohexene and cyclohexanone are important byproducts, the relative amounts of which are dependent on the catalyst structure, as shown in Table VIII. No dicyclohexyl could be detected. Cyclohexene is a product of oxidation under these conditions, since it is not present as an impurity in the reactant cyclohexane. [The cyclohexane used in this study was zoned-refined material, in which no cyclohexene could be detected by GC/MS analysis.] In order to determine the relative reactivity of cyclohexane, a competition experiment was carried out with styrene (cf. Table VII). With

the (3,3'-(OMe)<sub>2</sub>salen)Mn<sup>III</sup> complex **1b** as the catalyst, cyclohexane was found to be >300 times less reactive than styrene (see Experimental Section). Such a difference in reactivity is consistent with cyclohexene oxide arising from cyclohexene that is formed during the reaction. [Note the relative reactivity of cyclohexene and styrene is 1.0 under these conditions.]

**V. Isotopic Oxygen-18 Labeling Studies.** The course of the (salen)Mn<sup>III</sup>-catalyzed oxidation by iodosylbenzene was followed by isotopic oxygen-18 tracers. We used norbornene and cyclohexane as model substrates for olefin epoxidation and carbon-hydrogen activation, respectively.

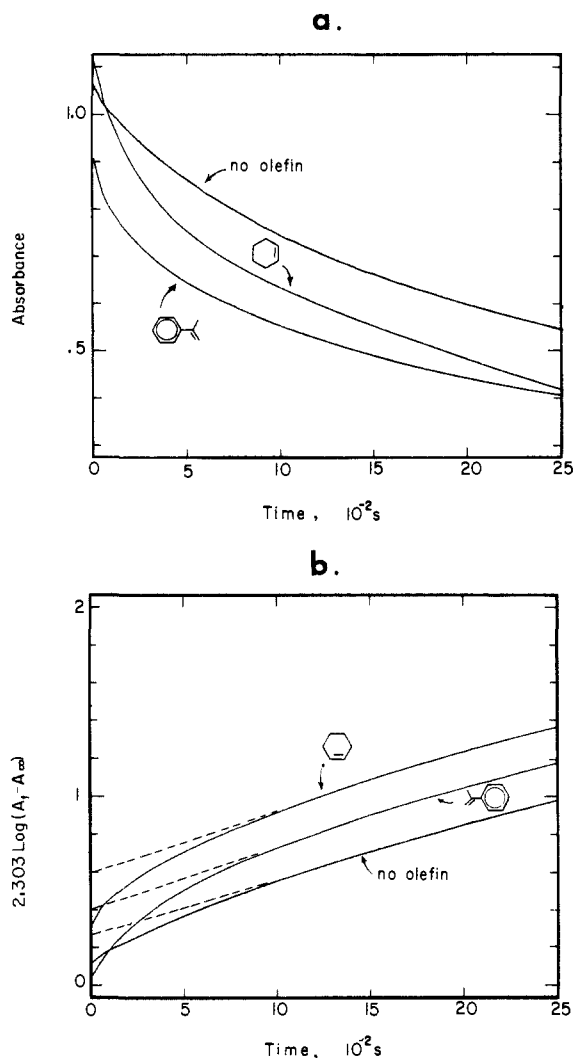
Oxygen-18 incorporation into norbornene could be readily followed by the increase in the *m/z* peak 112 as the parent molecule ion for norbornene oxide. When the epoxidation of norbornene with iodosylbenzene-<sup>18</sup>O (75% <sup>18</sup>O-enriched) was carried out under standard catalytic conditions,<sup>17</sup> the norbornene oxide also showed 75% oxygen-18 enrichment. Thus, epoxidation results from an oxygen-atom transfer from iodosylbenzene to the olefin. When the same reaction was carried out with 3.5 equiv of ordinary water (H<sub>2</sub><sup>16</sup>O) added relative to the iodosylbenzene charged, the oxygen-18 content was decreased to 32%. Conversely, if ordinary iodosylbenzene (PhI<sup>16</sup>O) was employed together with 3.5 equiv of isotopically enriched water (90% H<sub>2</sub><sup>18</sup>O), the product consisted of 26% norbornene oxide-<sup>18</sup>O. Moreover when the amount of enriched water was increased 10-fold to 35 equiv, the oxygen-18 enrichment rose to 74% in norbornene oxide. Oxygen-18 incorporation in the latter cases did not arise from prior equilibration of water with iodosylbenzene, since the unreacted iodosylbenzene upon recovery contained no isotopic label. We conclude that water must have been incorporated during the catalytic transfer from iodosylbenzene to the olefin substrate.

The (salen)Mn<sup>III</sup>-catalyzed oxidation of cyclohexane with iodosylbenzene-<sup>18</sup>O (75% enriched) under standard catalytic conditions<sup>17</sup> afforded *N*-cyclohexylacetamide containing 67% oxygen-18. However, this isotopic incorporation was completely washed out when the same oxidation was carried out in the presence of 3.5 equiv of ordinary water. The oppositely labeled combination of iodosylbenzene-<sup>16</sup>O with 3.5 equiv of enriched water afforded *N*-cyclohexylacetamide with an oxygen-18 content of 75%. Essentially the same isotopic results were obtained in the cyclohexanol and cyclohexene oxide fractions. Thus, the oxygen in these products arises from water, either that formed in the oxidation or that deliberately added.

**VI. (salen)Mn<sup>II</sup> as a Catalyst for Epoxidation.** In order to determine whether the neutral (salen)Mn<sup>II</sup> is also a catalyst for epoxidation, we compared its behavior relative to that of the cationic (salen)Mn<sup>III</sup>. Owing to the limited solubility of (salen)Mn<sup>II</sup> in acetonitrile, the comparison with (salen)Mn<sup>III</sup> was carried out by examining the relative reactivity of two pairs of olefins to each under comparable conditions. Despite its slower rate of catalysis, the competition experiments similar to those in Table VII indicate that (salen)Mn<sup>II</sup> is not distinguished from

(17) Standard conditions in this study are 0.30 mmol of olefin, 0.15 mmol of iodosylbenzene, and 0.011 mmol of catalyst in 5 mL of acetonitrile.

(18) See ref 6 and 7 and: (a) Smegal, J. A.; Hill, C. L. *J. Am. Chem. Soc.* **1985**, *105*, 3515. (b) Suslick, K.; Cook, B.; Fox, M. *J. Chem. Soc., Chem. Commun.* **1985**, 580.



**Figure 3.** Decay of the transient absorption derived from  $2.2 \times 10^{-3}$  M  $(5,5'-(\text{NO}_2)_2\text{salen})\text{Mn}^{\text{III}}$  and excess iodosylbenzene in acetonitrile in the absence of olefin and in the presence of either 0.03 M cyclohexene or 0.03 M  $\alpha$ -methylstyrene, as labeled. Change in (a) absorbance  $A$  and (b)  $\log(A_t - A_\infty)$  at 25 °C followed at  $\lambda$  680 nm in a 1-cm cuvette.

$(\text{salen})\text{Mn}^{\text{III}}$ . We interpret the same pattern of olefin reactivity to indicate a common catalytically active species, viz.,  $(\text{salen})\text{Mn}^{\text{III}}$ , which is undoubtedly formed by the partial oxidation of  $(\text{salen})\text{Mn}^{\text{II}}$  by iodosylbenzene.<sup>19</sup>

**VII. Kinetics of the Transient Spectral Band.** The transient spectral band with  $\lambda_{\text{max}} \sim 530$  nm in Figure 2 suggested the formation of a reactive intermediate, which we attempted to isolate in the following way. A solution of  $2 \times 10^{-3}$  M **1f** in acetonitrile was treated with a large excess of finely pulverized iodosylbenzene at 25 °C.<sup>20</sup> The dark brown mixture was stirred vigorously for 5 min and filtered directly into a pool of ether cooled to -40 °C. Low-temperature filtration afforded a dark brown solid **X** which was thermally quite labile and could not be recrystallized without decomposition. The absorption band at  $\lambda_{\text{max}}$  530 nm of the crude material dissolved in acetonitrile was the same as that observed in the catalytic system (see Figure 2).

The stability of the species **X** was quantitatively evaluated by monitoring the absorbance change at 680 nm. This decay rate

together with those obtained in the presence of added cyclohexene and  $\alpha$ -methylstyrene is shown in Figure 3a. The kinetics analysis based on first-order behavior is presented in Figure 3b.

### Discussion

The catalysis of olefin epoxidation by the cationic  $(\text{salen})\text{Mn}^{\text{III}}$  complexes is unique by comparison with similar transition-metal-catalyzed systems which are based either on the same metal and/or the same terminal oxidant. We employ four criteria to evaluate the catalytic effectiveness of the combination of  $(\text{salen})\text{Mn}^{\text{III}}$  and iodosylbenzene for epoxidation in eq 1. First, it is capable of epoxidizing quite a wide variety of diverse olefins in consistently good yields based on the utilization of the terminal oxidant (compare Table III). Second, the facile epoxidation of both cyclohexene and 1-octene is especially notable. It is well recognized that cyclohexene is prone to allylic oxidation, and the formation of cyclohexene oxide without serious competition from the production of cyclohexenol and cyclohexenone in Table II is unusual. Moreover terminal alkenes are usually among the least reactive olefins in metal-catalyzed epoxidations, yet 1-octene is readily formed from iodosylbenzene with the  $(\text{salen})\text{Mn}^{\text{III}}$  catalysts. Third, the oxygen-atom transfer to various olefins occurs with high stereochemical retention (Tables II and III).  $(Z)$ - $\beta$ -Methylstyrene and  $(Z)$ -stilbene are particularly useful test cases since oxygen-atom transfer to these *cis*-olefins often results in significant amounts of the rearranged *trans*-epoxides. Among the various  $(\text{salen})\text{Mn}^{\text{III}}$  cations, we find the electron-poor derivative with 5,5'-dinitro substituents to afford the highest stereospecificity in Table IV. Fourth, the relative reactivities of various olefins are encompassed in a very narrow range. Thus, only a factor of 10 separates the most reactive (*p*-methoxystyrene) from the least reactive (1-octene) olefin in Table VII.

**Oxomanganese(V) Species as the Reactive Intermediate.** The rapidity of the catalytic epoxidation coupled with the limited solubility of iodosylbenzene in acetonitrile precludes a rigorous examination of the kinetics of this system. Nonetheless the use of other mechanistic probes provides a reasonable understanding of how oxygen-atom transfer occurs. Thus, the spectral changes in Figure 2 demonstrate that the cationic  $(\text{salen})\text{Mn}^{\text{III}}$  catalyst reacts readily with iodosylbenzene to afford a new transient species **X** with  $\lambda_{\text{max}} \cong 530$  nm. The decay of this absorption band follows approximately first-order kinetics with a half-life of approximately 4 min at 25 °C, as shown in Figure 3. The presence of olefins such as cyclohexene and  $\alpha$ -methylstyrene leads to an apparent increase in the rate of disappearance of **X**.<sup>21</sup> However, a closer inspection of the rate profile shows that the difference lies only in the initial 10%. In particular, the logarithmic plot of the data in Figure 3b emphasizes the biphasic pattern to the decay kinetics. It clearly shows that the principal mode of decomposition is not dependent on the olefin. Therefore, **X** itself cannot be the reactive intermediate which is directly responsible for oxygen-atom transfer. This conclusion is also borne out by the observation that the catalytic epoxidation occurs at an *overall* rate which is much faster than the disappearance of **X** under comparable conditions.

We suggest that **X** is the  $\mu$ -oxomanganese(IV) dimer analogous to the ones previously isolated from manganese porphyrins by Hill and co-workers.<sup>22,23</sup> Such a formulation accords with the observation of essentially the same transient spectrum with another terminal oxidant, viz., *tert*-butyl hydroperoxide-pyridine.<sup>24</sup> Thus, the comparison in Figure 4 shows the new absorption band centered at 530–540 nm, the maximum of which is obscured by the tail of a strongly absorbing species at  $\lambda > 500$  nm. An inter-

(19) The (slight) differences in relative reactivity may be due to the apparently heterogeneous nature of the epoxidation induced by  $(\text{salen})\text{Mn}^{\text{III}}$ . Since this catalytic system is singularly bereft of anions and nucleophiles, the absence of sufficient amounts of a suitable counterion is probably responsible for the low solubility of  $(\text{salen})\text{Mn}^{\text{III}}$  formed under these conditions (by iodosylbenzene oxidation). The slow rate of the latter under these conditions accounts for the presence of insoluble, unreacted  $(\text{salen})\text{Mn}^{\text{II}}$  at the end of the epoxidation.

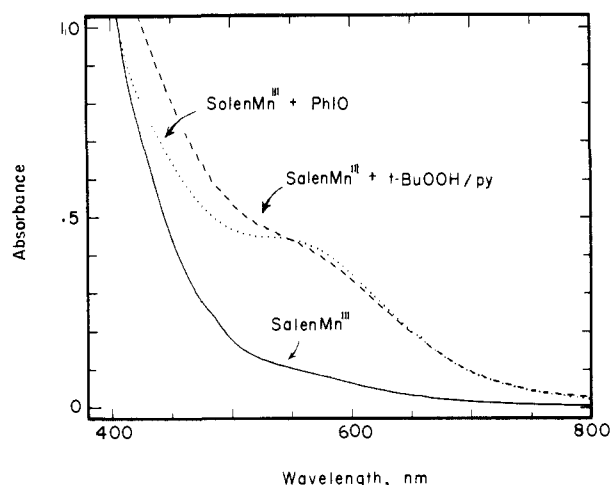
(20) At lower temperature this reaction is too slow to compete with decomposition (*vide infra*).

(21) The new band is bleached by olefins such as cyclohexene and  $\alpha$ -methylstyrene only to be replaced by the original absorption spectrum of the cationic  $(\text{salen})\text{Mn}^{\text{III}}$  precursor.

(22) (a) Schardt, B. C.; Hollander, F. J.; Hill, C. L. *J. Am. Chem. Soc.* **1982**, *104*, 3964. (b) Smegal, J. A.; Schardt, B. C.; Hill, C. L. *J. Am. Chem. Soc.* **1983**, *105*, 3510. (c) For a mononuclear  $\text{Mn}^{\text{IV}}$  species, see also: Camenzind, M. J.; Hollander, F. J.; Hill, C. L. *Inorg. Chem.* **1982**, *21*, 4301.

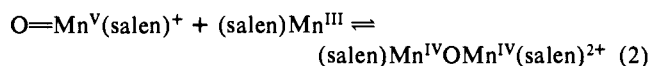
(23) The intermediate **X** is too unstable to isolate as a single crystal. Its formation from *tert*-butyl hydroperoxide-pyridine<sup>24</sup> indicates that it is not an iodosylbenzene adduct of the type described by Hill et al.<sup>22b</sup>

(24) Srinivasan, K.; Perrier, S.; Kochi, J. K. *J. Mol. Catal.*, in press.

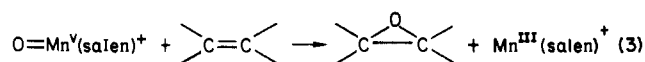


**Figure 4.** Comparison of the transient absorptions derived from mixing  $2.2 \times 10^{-3}$  M  $(5,5'-(\text{NO}_2)_2\text{salen})\text{Mn}^{\text{III}}$  in acetonitrile with (a) excess iodobenzene plus 1.25 M pyridine and (b) 0.06 M *tert*-butyl hydroperoxide plus 1.25 M pyridine at 25 °C.

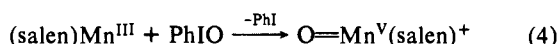
mediate which is common to both terminal oxidants is the active oxomanganese(V) species capable of readily coupling with (salen)Mn<sup>III</sup> to afford the species which we assign as  $\mu$ -oxomanganese(IV) (eq 2). The microscopic reverse process of eq



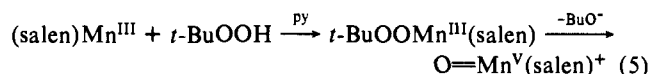
2 represents the disproportionation of the  $\mu$ -oxomanganese(IV) back to the active oxomanganese(V).<sup>25</sup> If such a disproportionation were relatively slow, it represents the rate-limiting step in the disappearance of X, owing to a rapid reaction of the active oxomanganese(V) species with olefin (eq 3). We account thus for the otherwise puzzling observation of a zero-order dependence of the decay rate with respect to the olefin (vide supra).



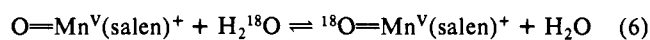
In this formulation, the active species responsible for oxygen-atom transfer to the olefin is the oxomanganese(V) cation in eq 3. Such a reactive intermediate is formed from iodobenzene by a process similar to that established for the related (salen)Cr<sup>III,5</sup> (eq 4) and from *tert*-butyl hydroperoxide-pyridine via an al-



kyperoxo intermediate<sup>24,26</sup> (eq 5). Indeed the comparison of the distinctive reactivity pattern of various olefins in catalytic oxidations<sup>24</sup> indicates that both of the oxomanganese(V) species



derived from these structurally diverse terminal oxidants are the same, as suggested in eq 4 and 5. Furthermore such an oxomanganese(V) intermediate is capable of isotopic exchange with <sup>18</sup>O-enriched water (eq 6), in comparison with the behavior of the

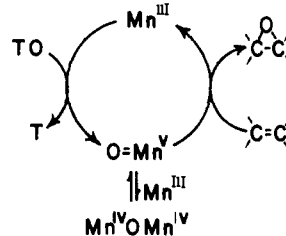


related oxochromium(V) cation noted earlier.<sup>5,27</sup> The facile

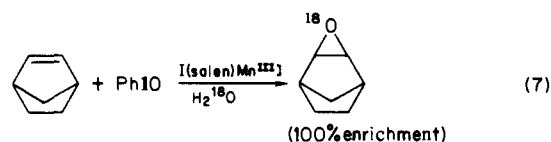
(25) (a) Reversibility of eq 2 would be enhanced if the  $\mu$ -oxomanganese(IV) dimer were to remain as a dicationic species, as depicted, owing to a singular absence of strongly coordinating anions or nucleophiles in this system.<sup>19</sup> (b) The initial, rapid process in Figure 4b may be attributed to the reactive oxomanganese(V) present in preequilibrium amounts in eq 2. The quantitative treatment of the complex kinetics is in progress.

(26) (a) Reference 1, p 56 ff. (b) Mimoun, H. In "The Chemistry of Peroxides"; Patai, S., Ed.; Wiley: New York, 1983; Chapter 15. (c) Groves, J. T.; Watanabe, Y.; McMurry, T. J. *J. Am. Chem. Soc.* **1983**, *105*, 4489. (d) For leading references, see also ref 10 and: Lee, W. A.; Bruce, T. C. *J. Am. Chem. Soc.* **1985**, *107*, 513.

## Scheme I



exchange in eq 6 accounts for the efficient <sup>18</sup>O-incorporation of labeled water into the epoxide during the catalytic process (eq 7) (see Results). Indeed the isotopic incorporation in eq 7 rep-



resents the best evidence for an independent oxomanganese species, since an alternative pathway via a prior exchange with the terminal oxidant<sup>28</sup> has been ruled out (vide supra).

The formation of the active oxomanganese(V) by either eq 4 or 5, coupled with the oxygen-atom transfer to olefin in eq 3, represents the oxygen-rebound mechanism for catalytic epoxidation, which was originally suggested by Groves and co-workers for iron(III) porphyrins and subsequently established with chromium(III) complexes.<sup>29</sup> In the case of the (salen)Mn<sup>III</sup> catalyst, the possibility of  $\mu$ -oxomanganese(IV) formation as in eq 2 leads to a diversion of the active oxomanganese(V). Such a competition for oxomanganese(V) would be serious only when the olefin is depleted (as in Figure 2)<sup>30</sup> or unreactive. However, the extent to which it is reversible (vide supra)<sup>25</sup> represents the catalytically viable system depicted in Scheme I, where TO is the terminal oxidant and Mn represents the (salen)Mn moiety. According to Scheme I, oxomanganese(IV) plays only an indirect, supportive role in the catalytic epoxidation—merely serving as an alternate source of the active oxomanganese(III) in eq 2. Accordingly, under static conditions such as those presented in Figure 2, it represents a more persistent form in which to park oxomanganese(V). Indeed the comparative studies of olefin reactivity indicate that the effectiveness of a catalytic system for oxygen-atom transfer based on the interconversion of  $\text{O}=\text{Mn}^{\text{IV}}(\text{salen})$  to (salen)Mn<sup>II</sup> is limited.<sup>32</sup>

**Oxygen-Atom Transfer from Oxomanganese(V).** Having formulated the active epoxidizing agent as  $\text{O}=\text{Mn}^{\text{V}}(\text{salen})^+$ , we now proceed with how it transfers its oxygen atom to the olefin. In such a complex, the salen ligand is highly susceptible to the presence of substituents (especially at the 5,5'-position or para

(27) Groves, J. T.; Kruper, W. J. *J. Am. Chem. Soc.* **1979**, *101*, 7613. (28) See, e.g., Burka, L. T.; Thorsen, A.; Guengerich, F. P. *J. Am. Chem. Soc.* **1980**, *102*, 7615. Guengerich, F. P.; MacDonald, T. L. *Acc. Chem. Res.* **1984**, *17*, 9.

(29) For leading references, see: (a) Groves, J. T.; Nemo, T. E.; Myers, R. S. *J. Am. Chem. Soc.* **1979**, *101*, 1032. Groves, J. T.; Nemo, T. E. *J. Am. Chem. Soc.* **1983**, *105*, 5786. (b) References 5 and 27.

(30) Under catalytic conditions, the buildup of oxomanganese(IV) dimer would be unfavored, especially at high olefin concentrations. Accordingly, the color change associated with the catalytic epoxidation with (salen)Mn<sup>III</sup> may be due to the transient oxomanganese(V). The spectral difference is difficult to distinguish since the absorption spectra of Mn<sup>IV</sup> and Mn<sup>V</sup> species are likely to be similar.<sup>31</sup>

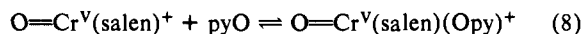
(31) Cf.: Carnieri, N.; Harriman, A.; Porter, G. *J. Chem. Soc., Dalton Trans.* **1982**, 931. Carnieri, N.; Harriman, A.; Porter, G.; Kalyanasundaram, K. *J. Chem. Soc., Dalton Trans.* **1982**, 1231.

(32) (a) The high reactivity of the catalytic system based on (salen)Mn<sup>III</sup> precludes the actual isolation and structure proof of the reactive epoxidizing agent. Accordingly, in the following discussion, we proceed with oxomanganese(V)  $\text{O}=\text{Mn}^{\text{V}}(\text{salen})^+$  as the reactive intermediate on the basis of the foregoing experimental evidence. (b) For an alternative of what may be a type of coordination (Lewis acid) catalysis, see: Van Atta, R. B.; Franklin, C. C.; Valentine, J. S. *Inorg. Chem.* **1984**, *23*, 4121. The isotopic <sup>18</sup>O incorporation in eq 7 does not support this possibility.

position to the ligating oxygens) which modulate its donor properties, as indicated by the variation of the redox potentials in Table I.<sup>33</sup> Accordingly we interpret the effect of 5,5'-dinitro groups on changing the epoxide yields and the pattern of relative reactivities of olefins (see Tables II and VI) as a reflection of a decreasing electron density in the oxomanganese(V) functionality.<sup>34</sup> The latter manifests itself in three ways. First, the attack of oxomanganese(V) on an olefinic center becomes less selective—so much so that there is little discrimination in Table VII between the electron-rich styrene, the strained norbornene, and a normal  $\alpha$ -olefin. Indeed only a rate factor of 10 separates *p*-methoxystyrene from 1-octene.<sup>35</sup> Second, the polar effect is shown by the trend in the reactivities of para-substituted styrenes which follow a Hammett correlation with a  $\rho$  value of only  $-0.3$ .<sup>36</sup> Third, the enhanced reactivity of oxomanganese(V) is sufficient to oxidize even such saturated hydrocarbons as cyclohexane. When taken together, these observations point to a radical-like character to the oxomanganese(V) functionality.

This conclusion differs from the electrophilic character of the related oxochromium(V) species  $\text{O}=\text{Cr}^{\text{V}}(\text{salen})^+$ .<sup>3</sup> Indeed the same three experimental criteria can be used to underscore the differences in reactivity between these isostructural oxometals. First, the attack of oxochromium(V) on an olefinic center is highly selective. The electron-rich *p*-methoxystyrene shows outstanding reactivity in contrast to  $\alpha$ -olefins which are unreactive—the difference representing a span of more than a factor of 1000. Second, the trend in reactivities of para-substituted styrenes follows a Hammett correlation with a significantly higher  $\rho$  value of  $-1.9$ . Third, saturated hydrocarbons such as cyclohexane are completely inert to oxochromium(V).

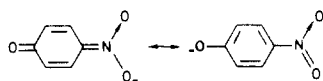
The difference in reactivity between oxomanganese(V) and oxochromium(V) is also shown by their sensitivity to added donor ligands. Thus, the presence of pyridine *N*-oxide enhances the reactivity of oxochromium(V) by several orders of magnitude via the formation of a six-coordinate adduct<sup>5</sup> (eq 8). By contrast,



the effect of ligands such as pyridine *N*-oxide, pyridine, and 4-(imidazol-1-yl)acetophenone on oxomanganese(V) is marginal at best (see Table V). The difference in sensitivity to donor ligaments may reflect the difference in the reactivity of these oxometals.

Despite such divergences in oxometal reactivities and behavior, they share in common the formation of the same series of by-products derived from skeletal rearrangements of various olefin substrates. Since control experiments rule out the subsequent isomerization of the first-formed epoxides, the coproduction of phenylacetaldehyde from styrene, phenylacetone from  $\beta$ -methylstyrene, and deoxybenzoin from stilbene must occur with both oxometals during the course of oxygen-atom transfer. The rearrangements observed with oxochromium(V) were previously interpreted as arising from a carbonium ion intermediate<sup>3</sup> (eq 9). Kinetic studies established that these cationic intermediates arose from the partitioning of a reactive precursor which was common with that leading to epoxide.<sup>3</sup>

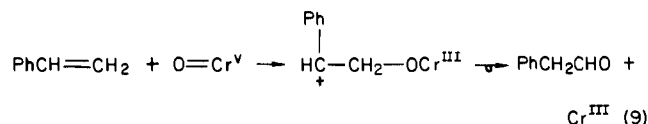
(33) The marked effect of 5,5'-dinitro groups on salen is analogous to the enhanced acidity of *p*-nitrophenol arising from added resonance stabilization such as



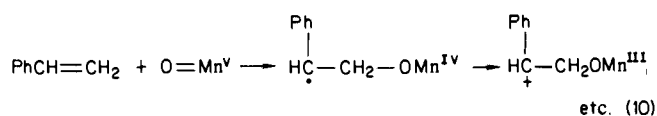
(34) In the related oxochromium(V) cations, this is reflected in an increase in the oxometal stretching frequency in the IR spectra.<sup>5,27</sup>

(35) Relative reactivities refer to the competition experiments in Table VII. Such measures of selectivity in oxygen-atom transfer pertain to the overall process including the preequilibrium formation of a precursor. Although the buildup of such an intermediate was not significant with  $\text{O}=\text{Cr}(\text{salen})^+$ ,<sup>3</sup> it could complicate the interpretation of selectivity in  $(\text{salen})\text{Mn}^{\text{III}}$  catalysis. (See discussion by Collman et al. in ref 8.)

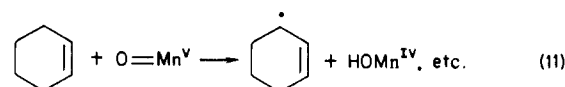
(36) A slightly better correlation is observed with  $\sigma^+$  substituent constants ( $\rho^+ 0.4$ ), but a distinction is unwarranted owing to the accuracy of the data and the limited number (four) of experimental points. For *p*-methoxystyrene, the aldehyde was assumed to be equivalent to the epoxide (see Table III).



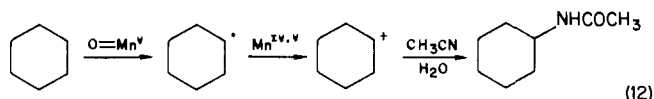
The way of reconciling similar cationic intermediates with the homolytic character of oxomanganese(V) described above is to postulate a competition from electron transfer within a similar intermediate<sup>37</sup> (eq 10). Whether a common precursor similar



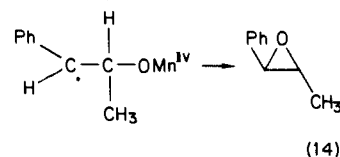
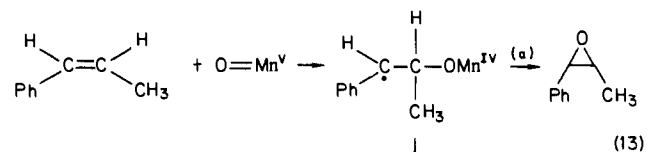
to that established with oxochromium(V) is partitioned with epoxide formation (eq 3) must await the development of kinetics evidence. Nonetheless, the viability of radical intermediates is shown by the allylic oxidation of cyclohexene and the attack on cyclohexane. Thus, the selective inhibition of cyclohexenol as a byproduct of cyclohexene epoxidation by the free radical trap ionol confirms its homolytic origin by a pathway such as



followed by either trapping with ionol or further oxidation. In the case of cyclohexane, the formation of cyclohexyl radicals by hydrogen-atom abstraction similar to that in eq 11 is followed by further oxidation to cyclohexanol.<sup>18</sup> The formation of *N*-cyclohexylacetamide in important amounts (Table VIII) represents the Ritter reaction and constitutes strong evidence for the oxidative formation of cyclohexyl cations (eq 12). Such an intermediate could also be responsible for the formation of cyclohexene and thus cyclohexene oxide.



The stereochemistry for oxygen-atom transfer to olefin is dependent on the electron density in the oxomanganese function, as reflected by the increasing trend for stereoselectivity to be optimized with electron-withdrawing substituents (Table IV). Such an observation can be accommodated within the radical intermediate in eq 13 if the rate of ring closure (a) relative to that



(37) (a) The diminution in the yields of cationic rearrangement products indicates that the rate of such an electron transfer is decreased by the added donor ligand pyridine. (b) It is interesting to note that the catalytic oxidation of (*Z*)- and (*E*)-stilbenes with  $(\text{salen})\text{Mn}^{\text{III}}$  also affords small but discrete amounts of diphenylacetaldehyde (Table III), which may result from homolytic rearrangement.<sup>38</sup> It is noteworthy that diphenylacetaldehyde was not detected with oxochromium(V) as the epoxidizing agent.<sup>3</sup> (c) The degradation of the catalyst does not appear to be directly related to these carbon-centered intermediates, since it occurs with iodosylbenzene in the absence of olefin. (d) Since the stereochemistry of epoxidation is not strongly influenced by pyridine, it must be determined in a step which is different from that leading to cationic rearrangement.

(38) Beckwith, A. L. J.; Ingold, K. U. In "Rearrangements in Ground and Excited States"; de Mayo, P., Ed.; Academic: New York, 1980; Vol. 1, Chapter 4. See also: Wilt, J. W. *Free Radicals*. 1973 1973, 1, 333.



of bond rotation (b) is controlled by the electron-deficient center on manganese. Indeed we observe the same trend in substituent effects on (salen)Mn<sup>III</sup> in determining the catalytic reactivity (Table III) as well as selectivity (Tables VI and VII) in oxygen-atom transfers to various olefins. Moreover it extends to the homolytic carbon-hydrogen activation of allylic (Table II) and saturated (Table VIII) carbon centers. As important as the substituent effect is in modulating the properties of (salen)Mn<sup>III</sup>, it leaves unanswered the question of whether the active oxomanganese species which we have formulated as O=Mn<sup>V</sup>(salen)<sup>+</sup> should not be represented as the charge-transfer isomer O=Mn<sup>IV</sup>(salen<sup>+</sup>).<sup>39</sup>

## Conclusion

Substituents effectively modulate the behavior of (salen)Mn<sup>III</sup> cations as distinctive catalysts among the various metal complexes which have been examined for olefin epoxidation. In a catalytic system based on iodosylbenzene as the terminal oxidant, the (salen)Mn<sup>III</sup> cation produces consistently high yields of epoxide from various olefinic substrates with high stereochemical control. The low substrate selectivity is attributed to a radical-like transition state for the step in which the oxygen atom is transferred. The latter is supported by a Hammett  $\rho$  value of only -0.3 for para-substituted styrenes and the observation of homolytic carbon-hydrogen activation. A combination of spectral, kinetics, and isotopic labeling studies points to an oxomanganese(V) species as the reactive intermediate serving as the key relay between the terminal oxidant and the olefin. However, the active oxomanganese(V) species can be tied up as  $\mu$ -oxomanganese(IV) dimers by the ready combination with manganese(III) cations. The extent to which such a conproportionation is reversible represents the viable catalytic system represented in Scheme I for olefin epoxidation.

## Experimental Section

**Materials.** Salicylaldehyde, ethylenediamine, and manganese acetate (Fisher); 5-nitrosalicylaldehyde (Eastman Kodak); and 5-chlorosalicylaldehyde, *o*-vanillin, and 5-methoxysalicylaldehyde (Aldrich Chemical Co.) were used as received. *o*-Hydroxybenzophenone was prepared by the Friedel-Crafts reaction of *o*-hydroxybenzoyl chloride with benzene.<sup>40</sup> 3,5-Dinitrosalicylaldehyde was made by nitrating salicylaldehyde.<sup>41</sup> 2,3-Diamino-2,3-dimethylbutane was prepared from 2,3-dimethyl-2,3-dinitrobutane by acidic reduction with granular tin, followed by distillation from KOH pellets.<sup>42</sup> Diethylenetriamine was a sample kindly donated by Shell Chemical Co.

Iodosylbenzene was prepared by the hydrolysis of the corresponding diacetate (Aldrich) with aqueous sodium hydroxide and stored at -20 °C.<sup>43</sup> Isotopically labeled iodosylbenzene-<sup>18</sup>O (75% enriched) was prepared in a previous study.<sup>7</sup> *m*-Chloroperoxybenzoic acid (*m*-CPBA 80-85%) was a commercial sample from Aldrich. 1-Octene, cyclohexene, cyclooctene, styrene, *p*-methoxy-, *p*-methyl-, and *p*-chlorostyrene,  $\alpha$ -methylstyrene, (*E*)- $\beta$ -methylstyrene, (*Z*)- $\beta$ -methylstyrene, (*E*)-stilbene, (*Z*)-stilbene, and norbornene were all commercial samples from Aldrich. *o,o'*-Dimethylstyrene was obtained from Fairfield Research Chemicals, and (*E*)- and (*Z*)-2-hexene were obtained from Wiley Organics.

1-Octene, *cis*-cyclooctene, norbornene, and (*E*)- and (*Z*)-2-hexene were distilled from lithium aluminum hydride under argon and stored in Schlenk vessels. All the styrenes were purified by distillation from lithium aluminum hydride under reduced pressure and stored at -20 °C in Teflon-stoppered Schlenk vessels under argon. (*E*)- and (*Z*)-stilbene were dissolved in hexane and chromatographed on a column of alumina. The solvent was removed under reduced pressure, and the pure olefins were stored at -20 °C. All the starting olefins were analyzed by gas chromatography. The presence of 4% cyclooctane in *cis*-cyclooctene was noted and confirmed by GC/MS analysis.

The majority of the epoxides were independently prepared by the epoxidation of corresponding alkenes with *m*-CPBA in methylene chlo-

ride.<sup>44</sup> *p*-Methoxystyrene oxide was prepared by the alkali treatment of *p*-methoxystyrene dibromide.<sup>45</sup> The epoxides were identified by their <sup>1</sup>H NMR spectra and confirmed by the GC/MS cracking patterns. The mass spectra were stored in the library of the GC/MS computer (vide infra) and retrieved when required for comparison purposes. Styrene oxide and cyclohexene oxide were commercial samples (Aldrich).

Hexane, acetonitrile, chlorobenzene, pyridine, diethyl ether, dimethyl sulfoxide, and dichloromethane were reagent grade commercial solvents which were repurified by standard methods.<sup>46</sup> After distillation, they were stored under an argon atmosphere in Schlenk flasks. Pure cyclohexane obtained as zone-refined material (J. Hinton, Valparaiso, FL; fluorescence < 0.2 ppb quinine base) was distilled from LiAlH<sub>4</sub> prior to use.

**Synthesis of Schiff Base Ligands.** The ligand salenH<sub>2</sub> was prepared by a literature procedure,<sup>47</sup> as were the 7,7'-diphenyl, 5,5'-dichloro, 5,5'-dinitro, 5,5'-dimethoxy, 3,3'-dimethoxy, 5,5'-dinitro-8,8,8',8'-tetramethyl, and 3,3',5,5'-tetranitro analogues. They were recrystallized from ethanol as bright yellow solids. Similarly, 5,5'-(NO<sub>2</sub>)<sub>2</sub>salenH<sub>2</sub> was obtained by the condensation of 5,5'-dinitrosalicylaldehyde and diethylenetriamine in ethanol.<sup>48</sup>

**General Procedure for the Synthesis of (salen)Mn<sup>II</sup> Complexes.**<sup>49-53</sup> Owing to their air-sensitivity, the manganese(II)-Schiff base complexes were prepared under argon with strict exclusion of air. To a suspension of the appropriate salenH<sub>2</sub> (4 mmol) in 40 mL of deaerated absolute ethanol was added a solution of KOH (8 mmol) dissolved in 10 mL of deaerated ethanol through a cannula needle. To the resulting yellow solution was added dropwise a solution of Mn<sup>II</sup>(OAc)<sub>2</sub>·4H<sub>2</sub>O (4 mmol) in 10 mL of deaerated methanol with the aid of a Teflon cannula. The yellow solution turned dark yellow or orange, and a yellow or orange solid began to appear. The solid suspension was stirred vigorously for 1 h at room temperature and refluxed for 3-4 h to ensure completion of the reaction. The solution was then cooled to room temperature, and the yellow precipitate was Schlenk-filtered, washed with deaerated methanol, and dried *in vacuo*. The yield, IR spectral data (Nujol mull), and magnetic susceptibility data of some of the manganese(II)-Schiff base complexes are given below. (salen)Mn<sup>II</sup>. Yield: 62%. IR: 1620 (s), 1525 (s), 1340 (m), 1276 (m), 1234 (s), 1198 (s), 1140 (s), 1120 (m), 1086 (s), 1042 (m), 982 (s), 940 (m), 905 (s), 855 (s), 750 (s), 732 (s) cm<sup>-1</sup>.  $\mu_{\text{eff}} = 6.13 \mu_{\text{B}}$ . (3,3'-(OMe)<sub>2</sub>salen)Mn<sup>II</sup>. Yield: 55%. IR: 1620 (s), 1590 (m), 1554 (s), 1400 (s), 1318 (s), 1209 (vs), 1180 (s), 1155 (s), 1106 (s), 1080 (m), 1045 (m), 998 (s), 980 (s), 964 (s), 920 (s), 858 (m), 786 (s), 740 (s), 720 (m), 660 (s) cm<sup>-1</sup>.  $\mu_{\text{eff}} = 5.95$ . (5,5'-(Cl)<sub>2</sub>salen)Mn<sup>II</sup>. Yield: 60%. IR: 1632 (s), 1590 (w), 1530 (m), 1335 (m), 1290 (s), 1130 (m), 1090 (m), 1083 (w), 1030 (s), 975 (w), 940 (w), 830 (s), 785 (s), 710 (m), 640 (s) cm<sup>-1</sup>.  $\mu_{\text{eff}} = 5.72 \mu_{\text{B}}$ . (5,5'-(NO<sub>2</sub>)<sub>2</sub>salen)Mn<sup>II</sup>. Yield: 85%. IR: 1638 (s), 1554 (s), 1554 (s), 1384 (s), 1306 (vs), 1248 (s), 1184 (m), 1135 (w), 1103 (s), 1078 (m), 1044 (m), 972 (w), 950 (m), 889 (m), 842 (m), 787 (m), 756 (m), 733 (m), 698 (s), 644 (m) cm<sup>-1</sup>.  $\mu_{\text{eff}} = 5.74 \mu_{\text{B}}$ . (3,3',5,5'-(NO<sub>2</sub>)<sub>4</sub>salen)Mn<sup>II</sup>. Yield: 90%. IR: 1641 (s), 1594 (s), 1559 (s), 1578 (s), 1497 (s), 1377 (s), 1313 (vs), 1225 (s), 1182 (m), 1109 (s), 1014 (s), 987 (m), 928 (m), 855 (s), 837 (w), 807 (s), 788 (m), 751 (m), 733 (m), 710 (s), 532 (s), 510 (s), 455 (s) cm<sup>-1</sup>.  $\mu_{\text{eff}} = 5.82 \mu_{\text{B}}$ . (5,5'-(NO<sub>2</sub>)<sub>2</sub>salien)Mn<sup>II</sup>. Yield: 80%. IR: 1642 (s), 1601 (s), 1554 (m), 1489 (s), 1472 (s), 1436 (m), 1392 (m), 1313 (vs), 1242 (m), 1191 (m), 1131 (w), 1103 (s), 1053 (w), 985 (w), 933 (w), 843 (m, br), 759 (m), 735 (w), 699 (s), 641 (m) cm<sup>-1</sup>. (7,7'-Ph<sub>2</sub>salen)Mn<sup>II</sup>. Yield: 73%. IR: 1580 (s), 1430 (s), 1300 (s), 1230 (s), 1150 (m), 1035 (m), 970 (w), 910 (w), 835 (s), 750 (s), 700 (m) cm<sup>-1</sup>.  $\mu_{\text{eff}} = 5.73 \mu_{\text{B}}$ . The synthesis of the other (salen)Mn<sup>II</sup> analogues is reported separately.<sup>24</sup>

**Structure of (7,7'-Ph<sub>2</sub>salen)Mn<sup>II</sup> by X-ray Crystallography.** A single orange crystal of (7,7'-Ph<sub>2</sub>salen)Mn<sup>II</sup> was grown from pyridine. A suitable crystal of dimensions 0.12 × 0.12 × 0.12 mm was cleaved, transferred to the goniostat under nitrogen, and cooled to -160 °C for characterization and data collection. A search of a limited hemisphere

(44) (a) Swern, D. *Org. React.* **1953**, *7*, 378. (b) Fieser, L. F.; Fieser, M. "Reagents for Organic Synthesis"; Wiley: New York, 1967; Vol. 1, pp 137-139.

(45) Guss, C. O. *J. Am. Chem. Soc.* **1952**, *74*, 2561.

(46) Perrin, D. D.; Armarego, W. L.; Perrin, D. R. "Purification of Laboratory Chemicals"; Pergamon Press: New York, 1980.

(47) Pfeiffer, P.; Breith, E.; Lubbe, E.; Tsumaki, T. *Ann.* **1933**, *503*, 84.

(48) See ref 4a.

(49) Dey, K. *J. Indian Chem. Soc.* **1971**, *48*, 641.

(50) Lewis, J.; Mabbs, F. E.; Weigold, H. *J. Chem. Soc.* **1968**, 1699.

(51) See ref 4d.

(52) Kessel, S. L.; Emerson, R. M.; Debrunner, P. G.; Hendrickson, D. M. *Inorg. Chem.* **1980**, *19*, 1170.

(53) Yarino, T.; Matsushita, T.; Masuda, I.; Shinra, K. *Chem. Commun.* **1970**, 1317.

(39) (a) Bortolini, O.; Meunier, B. *J. Chem. Soc., Chem. Commun.* **1983**, 1364. (b) A similar dichotomy exists in the iron porphyrins between O=Fe<sup>V</sup>(P) and O=Fe<sup>IV</sup>(P<sup>+</sup>). For leading references, see: Lee, W. A.; Calderwood, T. S.; Bruce, T. C. *Proc. Natl. Acad. Sci. U.S.A.* **1985**, *82*, 4301.

(40) Charlesworth, E. H.; Charleson, P. *Can. J. Chem.* **1968**, *46*, 1843.

(41) Hill, H.; Robinson, R. *J. Chem. Soc.* **1933**, 486.

(42) Sayre, R. *J. Am. Chem. Soc.* **1955**, *77*, 6090.

(43) Lucas, H. J.; Kennedy, E. R.; Formo, M. W. "Organic Synthesis"; Wiley: New York, 1955; Collect. Vol. III, p 483.

of reciprocal space located a set of reflections which could be indexed as  $C2/c$  with cell dimensions and other data as follows:  $a = 22.119$  (13) Å,  $b = 10.412$  (4) Å,  $c = 20.497$  (12) Å,  $\beta = 121.02$  (2)°,  $Z = 4$ , empirical formula  $MnC_{48}H_{42}O_3N_6$ ,  $V = 4045.72$  Å<sup>3</sup>,  $\rho_{\text{calcd}} = 1.297$  g cm<sup>-3</sup>, radiation Mo  $K\alpha$  ( $\lambda = 0.71069$  Å),  $fw = 789.84$ , linear absorption coefficient =  $3.525$  cm<sup>-1</sup>. The diffractometer utilized for data collection was designed and constructed locally:<sup>54</sup> collection range  $6^\circ < 2\theta < 45^\circ$ , scan speed =  $4^\circ/\text{min}$ , scan width =  $2^\circ + \text{dispersion}$ , total reflections collected =  $2870$  (2654 unique); independent data,  $F < 3\sigma(F) = 1954$ ,  $R(F) = 0.0549$ ,  $R_w(F) = 0.0518$ ; goodness of fit for last cycle =  $0.944$ ; max  $\Delta/\sigma$  for last cycle =  $0.05$ . Direct methods (MULTAN 78) located the position of the Mn atom on a crystallographic 2-fold axis at  $1/2, 0.0255, 1/4$ , as well as 12 other atoms. A difference Fourier phased on the above atoms located all the remaining non-hydrogen atoms. Hydrogen atoms were located in a difference Fourier phased on the non-hydrogen contributions. The trial structure was refined by full-matrix least-squares refinement (anisotropic thermal parameters for Mn, O, N, and C; isotropic for H). A final difference Fourier was featureless, the largest peak being  $0.21$  e Å<sup>-3</sup>. The structure appears well-ordered, and all hydrogen atoms converged to chemically realistic positions. The  $\psi$  scans of several reflections were essentially flat, and no absorption correction was performed. Tables of the fractional coordinates, bond distances, and bond angles are listed separately in the supplementary material.

**General Procedure for the Synthesis of [(salen)Mn<sup>III</sup>]<sup>+</sup>PF<sub>6</sub><sup>-</sup> Salts, 1a–e.** To a stirred suspension of the (salen)Mn<sup>II</sup> complex, in 20 mL of deaerated acetonitrile, a solution of ferricinium hexafluorophosphate (1 mmol) dissolved in 30 mL of acetonitrile was added dropwise via a Teflon cannula. The yellow suspension immediately began to turn brown. Stirring was continued for 30 min during which time the mixture became completely homogeneous. The solvent was removed under reduced pressure, and the neutral side product ferrocene was removed by several ether extractions. The manganese(III) complex which remained as a brown residue was crystallized from either a mixture of acetone and water or acetone and ethanol. The brown microcrystalline product was dried under vacuum for 2 h. The detailed data of characterization are provided below, for some representative examples. [(salen)Mn<sup>III</sup>]<sup>+</sup>PF<sub>6</sub><sup>-</sup> (1a). Yield: 60%. IR (Nujol): 3588 (br), 1618 (s), 1601 (s), 1551 (s), 1442 (s), 1391 (s), 1328 (m), 1281 (s), 1270 (s), 1247 (s), 1212 (s), 1156 (m), 1137 (s), 1090 (m), 1049 (m), 1032 (w), 980 (w), 952 (w), 905 (s), 836 (vs, br), 802 (s), 752 (s), 742 (s), 647 (m), 634 (m) cm<sup>-1</sup>. UV–vis in CH<sub>3</sub>CN [nm,  $\epsilon$  (M<sup>-1</sup> cm<sup>-1</sup>): 218 ( $3.06 \times 10^4$ ), 231 ( $3.63 \times 10^4$ ), 282 ( $1.60 \times 10^3$ ), 311 ( $1.12 \times 10^3$ ), 353 (7300), 402 (4500), 494 (1000).  $\mu_{\text{eff}} = 4.73$   $\mu_B$ . Anal. Calcd for C<sub>16</sub>H<sub>16</sub>O<sub>3</sub>N<sub>2</sub>MnPF<sub>6</sub>: C, 39.69%; H, 3.33%; N, 5.78%. Found: C, 39.66%; H, 3.30%; N, 5.72%. [(3,3'-(OMe)<sub>2</sub>salen)Mn<sup>III</sup>]<sup>+</sup>PF<sub>6</sub><sup>-</sup> (1b). Yield: 51%. IR (Nujol): 3400 (br), 1625 (s), 1605 (s), 1551 (s), 1470 (m), 1446 (s), 1436 (s), 1300 (s), 1257 (s), 1223 (s), 1090 (m), 1051 (w), 990 (m), 967 (m), 851 (vs, br), 778 (w), 750 (m), 733 (s), 651 (m), 619 (w) cm<sup>-1</sup>. UV–vis in CH<sub>3</sub>CN [nm,  $\epsilon$  (M<sup>-1</sup> cm<sup>-1</sup>): 303 ( $1.15 \times 10^3$ ), 335 ( $1.16 \times 10^3$ ), 382 (7340), 544 (1030).  $\mu_{\text{eff}} = 4.48$   $\mu_B$ . Anal. Calcd for C<sub>18</sub>H<sub>22</sub>N<sub>2</sub>O<sub>4</sub>PF<sub>6</sub>Mn: C, 38.45%; H, 3.94%; N, 4.98%. Found: C, 39.00%; H, 3.95%; N, 4.94%. [(5,5'-(OMe)<sub>2</sub>salen)Mn<sup>III</sup>]<sup>+</sup>PF<sub>6</sub><sup>-</sup> (1c). Yield: 40%. IR (Nujol): 1635 (s), 1616 (s), 1556 (s), 1472 (s), 1283 (s), 1253 (m), 1244 (m), 1165 (s), 1094 (m), 1053 (s), 1040 (s), 972 (m), 840 (vs, br), 770 (m), 727 (w), 619 (m) cm<sup>-1</sup>. [(5,5'-(Cl)<sub>2</sub>salen)Mn<sup>III</sup>]<sup>+</sup>PF<sub>6</sub><sup>-</sup> (1e). Yield: 68%. IR (Nujol): 1627 (s), 1539 (s), 1419 (w), 1328 (w), 1275 (s), 1262 (m), 1191 (m), 1098 (m), 1045 (m), 847 (vs, br), 804 (s), 712 (s) cm<sup>-1</sup>. UV–vis in CH<sub>3</sub>CN [nm,  $\epsilon$  (M<sup>-1</sup> cm<sup>-1</sup>): 283 ( $1.47 \times 10^4$ ), 350 (7320), 412 (4710), 506 (980).  $\mu_{\text{eff}} = 4.41$   $\mu_B$ . Anal. Calcd for C<sub>16</sub>H<sub>16</sub>O<sub>4</sub>N<sub>2</sub>PF<sub>6</sub>MnCl<sub>2</sub>: C, 33.62%; H, 2.80%; N, 4.90%. Found: C, 32.91%; H, 2.57%; N, 4.67%. [(7,7'-Ph<sub>2</sub>salen)Mn<sup>III</sup>]<sup>+</sup>PF<sub>6</sub><sup>-</sup> (1d). Yield: 60%. IR (Nujol): 3400 (br), 1598 (s), 1572 (s), 1532 (s), 1442 (m), 1327 (s), 1290 (m), 1237 (s), 1151 (s), 835 (vs), 739 (m), 702 (s), 636 (w) cm<sup>-1</sup>. UV–vis in CH<sub>3</sub>CN [nm,  $\epsilon$  (M<sup>-1</sup> cm<sup>-1</sup>): 238 ( $4.20 \times 10^4$ ), 280 ( $1.99 \times 10^4$ ), 313 ( $1.25 \times 10^4$ ), 356 (7970), 398 (5760), 498 (1020).  $\mu_{\text{eff}} = 4.42$   $\mu_B$ . Anal. Calcd for C<sub>28</sub>H<sub>28</sub>N<sub>2</sub>O<sub>3</sub>PF<sub>6</sub>Mn: C, 50.00%; H, 4.16%; N, 4.16%. Found: C, 50.39%; H, 4.14%; N, 4.07%.

**General Procedure for the Synthesis of [(salen)Mn<sup>II</sup>]<sup>+</sup>PF<sub>6</sub><sup>-</sup> Salts 1f and 1g.** To a suspension of the appropriate (salen)Mn<sup>II</sup> complex (4 mmol) in 50 mL of deaerated CH<sub>3</sub>CN was added a solution of ferrocenium hexafluorophosphate (4 mmol) in 100 mL of CH<sub>3</sub>CN through a Teflon cannula. The resulting greenish brown suspension was stirred for 1 h. The homogeneous solution was concentrated to 20 mL and poured onto a pool of ether (100 mL). The flocculent greenish brown precipitate was dissolved in an acetone–ethanol mixture, which on slow evaporation in air gave greenish brown needles of the product. The product was dried in vacuo for 2 h. [(5,5'-(NO<sub>2</sub>)<sub>2</sub>salen)Mn<sup>II</sup>]<sup>+</sup>PF<sub>6</sub><sup>-</sup> (1f). Yield: 61%. IR (Nujol): 3400 (br), 1631 (s), 1601 (s), 1560 (s), 1496 (m), 1440 (w),

1388 (s), 1330 (s), 1298 (vs), 1137 (w), 1109 (s), 989 (w), 954 (m), 916 (w), 860 (s), 845 (vs), 802 (s), 757 (m), 701 (m), 660 (m) cm<sup>-1</sup>. UV–vis in CH<sub>3</sub>CN [nm,  $\epsilon$  (M<sup>-1</sup> cm<sup>-1</sup>): 242 ( $2.86 \times 10^4$ ), 275 ( $2.74 \times 10^4$ ), 351 ( $2.34 \times 10^4$ ).  $\mu_{\text{eff}} = 4.65$   $\mu_B$ . Anal. Calcd for C<sub>19</sub>H<sub>21</sub>O<sub>7</sub>N<sub>4</sub>PF<sub>6</sub>Mn: C, 36.42; H, 3.35; N, 8.94. Found: C, 35.99; H, 3.46; N, 8.80. The dinitro analogue [(5,5'-(NO<sub>2</sub>)<sub>2</sub>-8,8',8''-(Me)salen)Mn<sup>II</sup>]<sup>+</sup>PF<sub>6</sub><sup>-</sup> (1g) was prepared by the same procedure. Yield: 45%. IR (Nujol): 1623 (sh, s), 1605 (s), 1554 (s), 1506 (m), 1341 (s), 1313 (s), 1148 (m), 1103 (m), 952 (m), 836 (vs, br), 804 (s), 755 (m), 662 (m) cm<sup>-1</sup>.

**Preparation of [(3,3',5,5'-(NO<sub>2</sub>)<sub>4</sub>salen)Mn<sup>II</sup>]<sup>+</sup>PF<sub>6</sub><sup>-</sup> (1h).** To a suspension of the manganese(II) complex (0.5 g, 1 mmol) in 50 mL of CH<sub>3</sub>CN was added a solution of (phen)<sub>3</sub>Fe<sup>3+</sup>(PF<sub>6</sub><sup>-</sup>)<sub>3</sub> (1.03 g, 1 mmol) in 50 mL of CH<sub>3</sub>CN via a Teflon cannula. The solution turned intense red immediately. The solvent was removed under reduced pressure, and the red complex (phen)<sub>3</sub>Fe<sup>2+</sup>(PF<sub>6</sub><sup>-</sup>)<sub>2</sub> was removed by extraction with CH<sub>2</sub>Cl<sub>2</sub>. The complete removal of the Fe<sup>II</sup> complex was indicated by the colorless methylene chloride extract. The brown residue was crystallized from an acetone–ethanol mixture to afford 0.45 g of the product 1h. Yield: 69%. IR (Nujol): 3500 (br), 1625 (s), 1600 (s), 1562 (s), 1628 (s), 1330 (vs), 1224 (m), 1105 (m), 984 (s), 924 (s), 835 (vs), 810 (s), 780 (s), 740 (m), 711 (s) cm<sup>-1</sup>. UV–vis in CH<sub>3</sub>CN [nm,  $\epsilon$  (M<sup>-1</sup> cm<sup>-1</sup>): 303 ( $2.56 \times 10^4$ ), 341 ( $2.43 \times 10^4$ ), 700 (745).  $\mu_{\text{eff}} = 4.20$   $\mu_B$ .

**Preparation of [(5,5'-(NO<sub>2</sub>)<sub>2</sub>saldien)Mn<sup>II</sup>]<sup>+</sup>PF<sub>6</sub><sup>-</sup> (1i).** To a suspension of the manganese(II) complex (1.11 mmol) in 25 mL of CH<sub>3</sub>CN was added a blue solution of (bpy)<sub>3</sub>Fe<sup>3+</sup>(PF<sub>6</sub><sup>-</sup>)<sub>3</sub> (1.1 mmol) in 50 mL of CH<sub>3</sub>CN via a Teflon cannula. The solution turned intense red immediately, owing to the formation of (bpy)<sub>3</sub>Fe<sup>2+</sup>. The solution was concentrated to 10 mL under reduced pressure, and then 100 mL of CH<sub>2</sub>Cl<sub>2</sub> was added to precipitate the complex, 1i, which was removed by filtration, washed several times with CH<sub>2</sub>Cl<sub>2</sub>, and dried in vacuo. Yield: 35%. IR (Nujol): 1653 (m), 1610 (s), 1558 (m), 1507 (m), 1339 (s), 1305 (s), 1103 (m), 948 (w), 847 (vs), 755 (w), 697 (w) cm<sup>-1</sup>. The preparation of the other cationic (salen)Mn<sup>III</sup> complexes is reported separately.<sup>24</sup>

**Instrumentation.** The electronic absorption spectra were recorded with a Hewlett-Packard 8450A diode-array spectrometer. Magnetic susceptibility was measured at 25 °C by the Evans method<sup>55</sup> in CD<sub>3</sub>CN [for Mn<sup>III</sup> complexes] and in Me<sub>2</sub>SO-*d*<sub>6</sub> [for Mn<sup>II</sup> complexes] by using a JEOL FX-90Q NMR spectrometer. Infrared spectra were obtained on a Nicolet DX-10 (Fourier transform) spectrometer. Cyclic voltammetry experiments were performed on a Princeton Applied Research Model 173 potentiostat/galvanostat equipped with a Model 176 current-to-voltage converter which provided a feedback compensation for ohmic drop between the working and reference electrodes. The voltammograms were recorded on a Houston Omnigraphic Series 2000 X–Y recorder.

Organic analyses were conducted on a Hewlett-Packard 5790 gas chromatograph with either a 12.5-m cross-linked dimethylsilicone capillary column or a 30-m Carbowax capillary column. The GC/MS analysis was performed on a Hewlett-Packard 5890 gas chromatograph interfaced to a Hewlett-Packard 5790B mass spectrometer (EI, 70 eV). In many instances, we found it possible to make direct comparisons with the same compounds listed in the 59973 NBS mass spectral library stored in the computer, hereafter referred to as the data station. In other cases, comparisons were made with those mass spectra of authentic samples. In every case, we found the mass spectra of *E* and *Z* isomers to be the same.

**Epoxidations of Olefins and the Analysis of Products.** The procedures for the oxidation of (*E*)-stilbene, (*Z*)-stilbene, and *p*-methoxystyrene are given in separate sections. All the other olefins were epoxidized by the procedure as follows: Epoxidation reactions were carried out under argon in a 25-mL Schlenk tube equipped with a stirring bar and an air-tight rubber septum. A stock solution of the ((NO<sub>2</sub>)<sub>2</sub>salen)Mn<sup>III</sup> complex 1f in acetonitrile ( $2.0 \times 10^{-3}$  M) was prepared, and 5 mL of this solution (corresponding to 0.01 mmol of the catalyst) was placed in the reaction tube which was previously evacuated and filled with argon. The olefin (0.3 mmol) and internal standard (0.30 mmol, consisting of either chlorobenzene, *n*-decane, or pentadecane) were added to the catalyst solution. Gas chromatography analysis was performed by withdrawing several aliquots with the aid of a hypodermic syringe. After the initial analysis, 33 mg (0.15 mmol) of iodosylbenzene was added in one lot to the reaction solution under a flow of argon. All of the iodosylbenzene usually disappeared within 5–15 min. The GC analysis was performed approximately 30 min after the start of the reaction. Quantification of the products was performed by the internal standard method in at least triplicate. The temperature program and the retention times (min) for alkenes and the products are given below. With a cross-linked dimethylsilicone capillary column (12.5 m), the retention times (min) were

(55) Evans, D. F. *J. Chem. Soc.* **1959**, 2003. See also: Jolly, W. L. "The Synthesis and Characterization of Inorganic Compounds"; Prentice-Hall: Englewood Cliffs NJ, 1971; pp 375–378.

as follows: at 100 °C, chlorobenzene (internal standard), 0.94; 1-octene, 0.83; 1-octene oxide, 1.65; iodobenzene, 1.89; at 60 °C programmed at 15 °C/min, cyclohexene, 0.74; cyclohexene oxide, 1.18; cyclohexenol, 1.31; *n*-decane (internal standard), 2.11; iodobenzene, 2.31; at 100 °C, norbornene, 0.74; norbornene oxide, 1.33; at 100 °C, (*Z*)- $\beta$ -methylstyrene, 1.45; (*E*)- $\beta$ -methylstyrene, 1.76; (*Z*)- $\beta$ -methylstyrene oxide, 2.45; (*E*)- $\beta$ -methylstyrene oxide, 2.55; phenylacetone, 2.59; at 105 °C, cyclooctene, 1.12; cyclooctane, 1.21; cyclooctene oxide, 2.25; at 100 °C,  $\alpha$ -methylstyrene, 1.45;  $\alpha$ -methylstyrene oxide, 2.27; phenylmethylacetaldehyde, 2.35; at 105 °C, *p*-chlorostyrene, 2.00; *p*-chlorostyrene oxide, 3.63; *p*-chlorophenylacetaldehyde, 3.40; at 100 °C, *p*-methylstyrene, 1.57; *p*-methylstyrene oxide, 3.48; *p*-methylphenylacetaldehyde, 2.76; at 105 °C, *o,o'*-dimethylstyrene, 2.06; *o,o'*-dimethylstyrene oxide, 3.77; at 60 °C (15 °C/min) (*E*)-2-hexene, 0.69; (*Z*)-2-hexene, 0.71; (*E*)-2-hexene oxide, 1.13; (*Z*)-2-hexene oxide, 1.25; at 100 °C, styrene, 1.05; styrene oxide, 2.01; phenylacetaldehyde, 1.83. With a Carbowax column (30 m), the retention times (min) were as follows: at 100 °C, styrene, 1.56; styrene oxide, 2.03; pentadecane (internal standard), 2.57; phenylacetaldehyde, 2.24; iodobenzene, 1.79. GC/MS analysis indicated that the formation of *exo*-norbornene oxide was contaminated by minor amounts of the endo isomer.

The mass spectral cracking patterns (EI, 70 eV) for the more distinctive byproducts are given below. Diphenylacetaldehyde, *m/z* (%): 51 (10), 63 (10), 115 (6), 139 (4), 152 (25), 153 (4), 163 (3), 165 (48), 167 (100), 168 (13). Deoxybenzoin, *m/z* (%): 50 (4), 51 (14), 63 (3), 65 (7), 77 (34), 78 (2), 91 (6), 105 (100), 106 (7), 196 (2).  $\alpha$ -Phenylpropionaldehyde, *m/z* (%): 50 (8), 51 (17), 77 (29), 78 (9), 79 (29), 91 (9), 103 (16), 105 (100), 106 (9), 134 (9). Phenylacetone, *m/z* (%): 39 (11), 43 (100), 50 (3), 51 (5), 63 (6), 65 (12), 89 (3), 91 (25), 92 (11), 134 (5).

**Epoxidation of (*E*)- and (*Z*)-Stilbenes Catalyzed by the ((NO<sub>2</sub>)<sub>2</sub>salen)Mn<sup>III</sup> Complex 1f.** The catalytic epoxidations of (*E*)- and (*Z*)-stilbenes were carried out with 33 mg (0.15 mmol) of iodosylbenzene suspended in a solution containing 0.3 mmol of either (*E*)- or (*Z*)-stilbene and 0.01 mmol of catalyst (as 5 mL of solutions of 2.1 × 10<sup>-3</sup> M 1f in acetonitrile). The suspension was stirred vigorously. No internal standard was added at this point. After 1 h, the solvent was removed under reduced pressure. To the brown residue 5 mL of anhydrous ether was added, followed by 0.029 mmol of diphenylethylene as the internal standard. The ether solution was carefully filtered through a Teflon cannula into another Schlenk tube. Ether was removed under reduced pressure. The residue was then dissolved in 0.4 mL of CDCl<sub>3</sub> (with 1% Me<sub>4</sub>Si) and an NMR spectrum taken. From the values of integration, the amounts of the different products were determined. The singlet resonances for the epoxide protons of (*Z*)-stilbene oxide and (*E*)-stilbene oxide occurred at  $\delta$  4.34 and 3.85, respectively. The methylene protons of diphenylethylene appeared as a singlet at  $\delta$  5.45. The singlet resonance at  $\delta$  4.26 was due to deoxybenzoin, PhCH<sub>2</sub>COPh, and the two doublets at  $\delta$  4.86 (*J* = 2.4 Hz) and 9.92 (*J* = 2.4 Hz) were assigned to (Ph)<sub>2</sub>CHCHO (vide infra for MS).

**Epoxidation of *p*-Methoxystyrene Catalyzed by the ((NO<sub>2</sub>)<sub>2</sub>salen)-Mn<sup>III</sup> Complex 1f.** The catalytic epoxidation of *p*-methoxystyrene was carried out with 33 mg (0.15 mmol) of PhIO suspended in a 5-mL CH<sub>3</sub>CN solution containing 0.3 mmol of *p*-methoxystyrene and 0.010 mmol of catalyst 1f. The suspension was stirred vigorously. After 1 h, the solvent was removed under reduced pressure. To the brown residue 5 mL of anhydrous ether was added followed by 0.032 mmol of diphenylethylene as the internal standard. The ether solution was carefully filtered via a cannula into a Schlenk tube. After the removal of ether on a rotary evaporator, the residue was dissolved in 0.4 mL of CDCl<sub>3</sub> (containing 1% Me<sub>4</sub>Si), and an NMR spectrum was recorded. No epoxide resonances were observed; instead a triplet at  $\delta$  9.70 (*J* = 2.44 Hz) and a doublet at  $\delta$  3.61 (*J* = 2.44 Hz) were observed. These resonances were assigned to *p*-methoxyphenylacetaldehyde by comparison with the resonance of an authentic sample. The *p*-methoxyphenylacetaldehyde was also identified by GC/MS analysis.

**Relative Reactivities of Olefins by Intermolecular Competitions.** The relative reactivities by intermolecular competition were calculated by the expression

$$k_X/k_Y \cong 2.3 \log (X_f/X_i) / \log (Y_f/Y_i)$$

where *X<sub>i</sub>* and *X<sub>f</sub>* are the initial concentrations of the olefins X and Y and *Y<sub>i</sub>* and *Y<sub>f</sub>* are the final concentrations of these olefins.<sup>56</sup> The ratio *k<sub>X</sub>*/*k<sub>Y</sub>* can also be calculated by the approximation

$$k_X/k_Y \cong (\Delta P/X_i) / (\Delta Q/Y_i)$$

where  $\Delta P$  and  $\Delta Q$  are the amounts of products from X and Y, respectively, and *X<sub>i</sub>* and *Y<sub>i</sub>* are the initial concentrations of the two olefins. For applying these equations, the initial concentrations of olefins were at least 5 times greater than the conversion. In a typical procedure for the competitive catalytic epoxidation, 0.3 mmol of each of the two olefins was mixed in a solution containing 0.01 mmol of complex 1f and 0.3 mmol of internal standard in 5 mL of CH<sub>3</sub>CN. Before the start of the reaction, the amounts of olefins were determined by GC analysis. Then, 0.15 mmol of iodosylbenzene was added and the solution vigorously stirred until all of it disappeared. The amounts of products formed and olefins consumed were determined by GC analysis. The original amounts of olefins and the amounts of olefins consumed are given in Table VII. The relative reactivities are calculated by the first equation above. The relative reactivity of (*Z*)-stilbene vs. (*E*)-stilbene was determined from NMR analysis by using a procedure similar to that used for determining yields of stilbene oxides. The consumption of olefins was calculated by using the two values of integration of the methylene singlet resonances of (*E*)-stilbene ( $\delta$  7.07) and (*Z*)-stilbene ( $\delta$  6.56). The relative reactivity of (*Z*)-stilbene vs. styrene was determined by GC analysis of olefins before and after the reaction using the dimethylsilicone glass capillary column (12.5 m) and chlorobenzene as the internal standard. The retention times were as follows: at 100 °C for 0.5 min, then programmed at 15 °C/min, styrene, 1.05 min; *cis*-stilbene, 5.24 min.

**Relative Reactivity of Styrene and Cyclooctene in Catalytic Epoxidations.** Since the competition method required the concentration of olefins (*X<sub>i</sub>* and *Y<sub>i</sub>*) to be 5–6 times larger than the conversion during the reaction, we employed large concentrations of styrene and cyclooctene. The amounts are given in Table VI. As earlier, iodosylbenzene (0.18 mmol) was added to a solution containing the mixture of olefins and 0.011 mmol of either the (salen)Mn<sup>+</sup> complex 1a or the ((NO<sub>2</sub>)<sub>2</sub>salen)Mn<sup>+</sup> complex 1f. The amounts of products formed were carefully determined by GC analysis, and these values are shown in Table VI.

Similarly, the relative reactivity of the cyclohexene–1-octene pair was determined by employing the several catalysts listed in Table VI.

**Stability of Styrene Oxide to the Reaction Conditions of Epoxidation.** To 5 mL of acetonitrile containing 1-octene (0.296 mmol), the ((NO<sub>2</sub>)<sub>2</sub>salen)Mn<sup>III</sup> complex 1f (0.011 mmol), chlorobenzene (internal standard, 0.294 mmol), and styrene oxide (0.089 mmol) was added 33 mg (0.15 mmol) of iodosylbenzene. After completion, the amounts of octene oxide and styrene oxide were found to be 0.086 and 0.089 mmol, respectively, as found by GC analysis. The amount of styrene oxide was unchanged and thus unaffected by the reaction conditions. The yield of octene oxide (59%) was similar to that found in the absence of styrene oxide.

Similar experiments were carried out to check the stability of (*Z*)- $\beta$ -methylstyrene oxide and cyclohexene oxide during the catalytic oxidation of 1-octene by PhIO with [(salen)Mn]<sup>+</sup>PF<sub>6</sub><sup>-</sup> (1a). The amounts of (*Z*)- $\beta$ -methylstyrene oxide (0.066 mmol) and cyclohexene oxide (0.075 mmol) remained unchanged after the reaction. The yield of octene oxide (0.044 mmol, 30% yield) was also not affected. In another experiment the stability of (*Z*)-stilbene oxide was established as follows. To 5 mL of acetonitrile containing 1-octene (0.296 mmol), the complex 1f (0.011 mmol), and (*Z*)-stilbene oxide (0.054 mmol) was added 0.15 mmol of PhIO. The reaction mixture was vigorously stirred, and after all of the PhIO had disappeared, the solvent was removed under reduced pressure. To the brown residue 5 mL of ether was added followed by 0.034 mmol of diphenylethylene. The ether solution is carefully filtered through a cannula. Ether was removed on a rotary evaporator, and the residue was dissolved in 0.4 mL of CDCl<sub>3</sub> (with 1% Me<sub>4</sub>Si) and a <sup>1</sup>H NMR spectrum recorded. From an inspection of the spectrum, it was clear that no deoxybenzoin or diphenylacetaldehyde were formed. The values of integration showed that (*Z*)-stilbene oxide had been recovered nearly quantitatively, i.e., 0.043 mmol (80%).

The stereochemical stability of olefins under reaction conditions was also shown by the absence of (*E*)- $\beta$ -methylstyrene and (*E*)-stilbene in the recovered fractions from (*Z*)- $\beta$ -methylstyrene and (*Z*)-stilbene, respectively.

**Olefin Epoxidation with (salen)Mn<sup>III</sup> Catalyst.** The catalytic epoxidations were carried out with 0.011 mmol of 1a, 0.30 mmol of olefin, and 0.15 mmol of iodosylbenzene at 25 °C as described above. Styrene yielded 0.055 mmol (38%) of epoxide and 0.015 mmol of phenylacetaldehyde. (*Z*)- $\beta$ -Methylstyrene yielded 0.051 and 0.006 mmol of (*Z*)- and (*E*)-epoxides and 0.020 mmol of phenylacetone. (*Z*)-Stilbene yielded 0.030 and 0.012 mmol of (*Z*)- and (*E*)-epoxides, 0.012 mmol of deoxybenzoin, and 0.009 mmol of diphenylacetaldehyde. (*E*)-Stilbene yielded 0.066 and <0.001 mmol of (*E*)- and (*Z*)-epoxides, <0.002 mmol of deoxybenzoin, and <0.002 mmol of diphenylacetaldehyde. Cyclohexene afforded 0.077 mmol of epoxide and 0.005 mmol of cyclohexenol. (*Z*)-2-Hexene yielded 0.094 and 0.003 mmol of (*Z*)- and (*E*)-epoxides.

(56) Moss, R. A. In "Carbenes"; Jones, M., Jr., Moss, R. A., Eds.; Wiley: New York, 1973; Vol. 1, pp 153–156. Also see: Poutsma, M. L. In "Free Radicals"; Kochi, J. K., Ed.; Wiley: New York, 1973; Vol. 2, pp 116–118.

(*E*)-2-Hexene yielded 0.035 and <0.001 mmol of (*E*)- and (*Z*)-epoxides. 1-Octene yielded 0.043 mmol of octene oxide.

**Oxidation of Cyclohexane by Iodosylbenzene Catalyzed by [(salen)-Mn]PF<sub>6</sub> Complexes.** Oxidation of cyclohexane was carried out with 33 mg (0.015 mmol) of iodosylbenzene suspended in a solution containing 600 μL of cyclohexane, 0.011 mmol of catalyst, and 0.010 mmol of internal standard tetradecane in 5 mL of CH<sub>3</sub>CN. The reaction solution was stirred vigorously. Usually the PhIO disappeared completely within a 15-min period. The solution was analyzed as before by GC, employing a Carbowax capillary column (30 m). The amounts of cyclohexanone, cyclohexanol, and cyclohexene oxide were calculated by the internal standard method and are given in Table VIII. For the observation of *N*-cyclohexylacetamide and cyclohexene, a dimethylsilicone capillary column was used. The retention times of cyclohexanone and cyclohexanol with a Carbowax column were 2.1 and 2.2 min, respectively, at 90 °C programmed at 10 °C/min. The retention times of cyclohexene and cyclohexylacetamide with the dimethylsilicone capillary column were 0.77 and 6.64 min, respectively, at 70 °C programmed at 15 °C/min. The identity of these compounds was confirmed by GC/MS analysis (data station). The relative reactivity of cyclohexane and styrene was measured by the competition method by the addition of 5.55 and 0.070 mmol, respectively, under standard catalytic conditions.<sup>17</sup> From the amounts of styrene oxide (0.031 mmol) relative to cyclohexene oxide (0.0053 mmol), *N*-cyclohexylacetamide (0.013 mmol), cyclohexanol, and cyclohexanone (0.0074 mmol), a lower limit of 300 was evaluated for the relative reactivity.

**Oxidations by Iodosylbenzene-<sup>18</sup>O Catalyzed by [(salen)Mn<sup>III</sup>]<sup>+</sup>PF<sub>6</sub><sup>-</sup> (1a).** The same procedures as given for the oxidations described above were used for PhI<sup>18</sup>O (~75% enriched label), in which the products were analyzed by GC/MS. The <sup>18</sup>O isotopic incorporation in the products was readily apparent from the mass spectral pattern. Quantitative analysis of <sup>18</sup>O incorporation was obtained from the relative abundance of the molecule/ion *M* + 2. For example, in the case of *N*-cyclohexylacetamide, the ratio of *m/z* 143 to *m/z* 141 (which corresponds to the unlabeled amide) was found to be that given in the Results. Similarly, the incorporation of oxygen-18 into the catalytic epoxidation was evaluated by the mass spectral peaks *m/z* 112 and 110 for the labeled and unlabeled norbornene oxide, respectively. Isotopically enriched water (90% H<sub>2</sub><sup>18</sup>O, Aldrich) was used in the exchange studies.

**Acknowledgment.** We thank S. Perrier for helpful discussions and invaluable technical assistance, J. C. Huffman for the X-ray crystal structure in Figure 1, the French Ministry of External

Affairs for a fellowship (P. Michaud), and the National Science Foundation and the Robert A. Welch Foundation for financial support.

**Registry No.** **1a**, 101142-76-1; **1b**, 101032-19-3; **1c**, 101032-21-7; **1d**, 101032-23-9; **1e**, 101054-47-1; **1f**, 101032-25-1; **1g**, 101032-27-3; **1h**, 101032-29-5; **1i**, 101032-31-9; (salen)Mn<sup>II</sup>, 36026-26-3; (3,3'-(OMe)<sub>2</sub>salen)Mn<sup>II</sup>, 101032-14-8; (5,5'-(Cl)<sub>2</sub>salen)Mn<sup>II</sup>, 23324-43-8; (5,5'-(NO<sub>2</sub>)<sub>2</sub>salen)Mn<sup>II</sup>, 42731-12-4; (3,3',5,5'-(NO<sub>2</sub>)<sub>4</sub>salen)Mn<sup>II</sup>, 101032-15-9; (5,5'-(NO<sub>2</sub>)<sub>2</sub>saldien)Mn<sup>II</sup>, 101032-16-0; (7,7'-(Ph)<sub>2</sub>salen)Mn<sup>II</sup>, 101032-17-1; (5,5'-(MeO)<sub>2</sub>salen)Mn<sup>II</sup>, 101032-32-0; (5,5'-(NO<sub>2</sub>)<sub>2</sub>-8,8',8'-(Me)<sub>4</sub>salen)Mn<sup>II</sup>, 101032-33-1; (bpy)<sub>3</sub>Fe<sup>3+</sup>(PF<sub>6</sub><sup>-</sup>)<sub>3</sub>, 28190-88-7; (phen)<sub>3</sub>Fe<sup>3+</sup>(PF<sub>6</sub><sup>-</sup>)<sub>3</sub>, 28277-57-8; (7,7'-Ph<sub>2</sub>salen)Mn(py)<sub>2</sub>, 101032-13-7; PhCH<sub>2</sub>CHO, 122-78-1; 4-MeC<sub>6</sub>H<sub>4</sub>CH<sub>2</sub>CHO, 104-09-6; 4-MeOC<sub>6</sub>H<sub>4</sub>CH<sub>2</sub>CHO, 5703-26-4; 4-ClC<sub>6</sub>H<sub>4</sub>CH<sub>2</sub>CHO, 4251-65-4; PhCH(CH<sub>3</sub>)CHO, 93-53-8; 2,6-(CH<sub>3</sub>)<sub>2</sub>C<sub>6</sub>H<sub>3</sub>CH<sub>2</sub>CHO, 27843-11-4; PhCH<sub>2</sub>COCH<sub>3</sub>, 103-79-7; PhCH<sub>2</sub>COPh, 451-40-1; Ph<sub>2</sub>CHCHO, 947-91-1; CH<sub>2</sub>=CH(CH<sub>2</sub>)<sub>5</sub>CH<sub>3</sub>, 111-66-0; PhCH=CH<sub>2</sub>, 100-42-5; 4-MeC<sub>6</sub>H<sub>4</sub>CH=CH<sub>2</sub>, 622-97-9; 4-MeOC<sub>6</sub>H<sub>4</sub>CH=CH<sub>2</sub>, 637-69-4; 4-ClC<sub>6</sub>H<sub>4</sub>CH=CH<sub>2</sub>, 1073-67-2; PhC(CH<sub>3</sub>)=CH<sub>2</sub>, 98-83-9; 2,6-(CH<sub>3</sub>)<sub>2</sub>C<sub>6</sub>H<sub>3</sub>CH=CH<sub>2</sub>, 2039-90-9; (*Z*)-PhCH=CHCH<sub>3</sub>, 766-90-5; (*E*)-PhCH=CHCH<sub>3</sub>, 873-66-5; (*Z*)-PhCH=CHPh, 645-49-8; (*E*)-PhCH=CHPh, 103-30-0; (*Z*)-CH<sub>3</sub>(CH<sub>2</sub>)<sub>2</sub>CH=CHCH<sub>3</sub>, 7688-21-3; (*E*)-CH<sub>3</sub>(CH<sub>2</sub>)<sub>2</sub>CH=CHCH<sub>3</sub>, 4050-45-7; ferricinium hexafluorophosphate, 11077-24-0; cyclohexenyl methyl ether, 39723-61-0; iodosylbenzene-<sup>18</sup>O, 80572-92-5; 4-methylstyrene oxide, 13107-39-6; 4-chlorostyrene oxide, 2788-86-5; 2,6-dimethylstyrene epoxide, 78924-72-8; (*Z*)-β-methylstyrene oxide, 4541-87-1; (*E*)-β-methylstyrene oxide, 23355-97-7; (*Z*)-stilbene oxide, 1689-71-0; (*E*)-stilbene oxide, 1439-07-2; (*Z*)-1-hexene oxide, 6124-90-9; (*E*)-1-hexene oxide, 6124-91-0; 4-(imidazol-1-yl)acetophenone, 10041-06-2; cyclohexene oxide, 286-20-4; 1-octene oxide, 2984-50-1; iodosylbenzene, 536-80-1; cyclooctene, 931-88-4; norbornene, 498-66-8; styrene oxide, 96-09-3; α-methylstyrene oxide, 2085-88-3; cyclooctene oxide, 286-62-4; pyridine, 110-86-1; pyridine *N*-oxide, 694-59-7; cyclohexane, 110-82-7; cyclohexanol, 108-93-0; acetylaminocyclohexane, 1124-53-4; cyclohexanone, 108-94-1; cyclohexene, 110-83-8; 2-cyclohexenol, 822-67-3; norbornene oxide, 278-74-0.

**Supplementary Material Available:** Tables of fractional atomic coordinates, bond distances, and bond angles for (7,7'-Ph<sub>2</sub>salen)Mn(py)<sub>2</sub> (3 pages). Ordering information is given on any current masthead page.